



Cite this: *Green Chem.*, 2025, **27**, 4016

## Technological advances in ligninolytic enzymes for the biological valorization of lignin

Ning Fu,<sup>a,b,c</sup> Ruo-Ying Liu,<sup>a,b,c</sup> Ya Zhou,<sup>a,b,c</sup> Bing-Zhi Li,<sup>ID \*</sup><sup>a,b,c</sup> Ying-Jin Yuan,<sup>ID</sup><sup>a,b,c</sup> and Zhi-Hua Liu <sup>ID \*</sup><sup>a,b,c</sup>

Lignin is a promising renewable aromatic resource with significant potential for conversion into high-value products, making it a key component in advancing biorefinery processes and supporting the bioeconomy. However, its structural heterogeneity and macromolecular complexity pose major challenges to its biological valorization. This work focuses on advancing the bio-depolymerization of lignin into highly bioavailable derivatives for downstream biocatalysis by exploring cutting-edge technologies for the screening and modification of ligninolytic enzymes. Key enzymes involved in both extracellular depolymerization and intracellular transformation of lignin serve as critical targets for advancing its biological valorization. A range of state-of-the-art technologies can be employed for high-throughput screening of efficient ligninolytic enzymes or bacteria, thereby enriching the pool of available biocatalysts. Protein engineering offers a powerful approach for developing artificial enzymes with industrial production advantages. Additionally, artificial intelligence provides valuable strategies for designing and modifying ligninolytic enzymes. Overall, the interdisciplinary application of these advanced technologies is instrumental in propelling lignin biological valorization to a more sophisticated stage of green development.

Received 9th November 2024,

Accepted 3rd March 2025

DOI: 10.1039/d4gc05724d

rsc.li/greenchem

### Green foundation

1. This work highlights recent advancements in biological lignin valorization using ligninolytic enzymes and cutting-edge technologies in the field. The interdisciplinary application of these innovations plays a crucial role in advancing lignin biological valorization, driving it toward a more sustainable stage of green chemistry development.
2. Lignin is the largest renewable source of aromatics in nature. A thorough review of cutting-edge technologies could advance the biological valorization of lignin, potentially transforming its utilization and contributing to biorefining and the bioeconomy.
3. Future work will focus on scaling the practical applications of advanced technologies for discovering and optimizing ligninolytic enzymes and microbial strains. Enhancements in the robustness, efficiency, and specificity of these biological systems will unlock new research opportunities and establish a foundation for developing greener, more sustainable methods for industrial lignin valorization.

## 1. Introduction

Lignin, one of the three major components of lignocellulosic biomass (LCB), is the most abundant terrestrial aromatic biopolymer.<sup>1</sup> Lignin is an underutilized renewable energy source and holds great promise as an alternative aromatic material for value-added products in biological manufacturing.<sup>2–4</sup> Its utilization can significantly reduce the dependence on non-renewable fossil fuels, such as petroleum derived aromatic hydrocarbons.<sup>5,6</sup> Despite this potential, lignin is a highly

heterogeneous biopolymer.<sup>2</sup> Its proportion varies among different lignocellulosic biomasses and is closely related to the proportions of cellulose and hemicellulose.<sup>7</sup> Lignin is typically composed of three subunits: guaiacyl (G), syringyl (S), and *p*-hydroxyphenyl (H), which polymerize *via* C–C or C–O linkages.<sup>8</sup> Therefore, the structural heterogeneity and macromolecular characteristics of lignin polymers, composed of different subunits, are major obstacles to their biological valorization.<sup>5</sup> To overcome the obstacles posed by these inherent features, it is crucial to develop a wide range of deconstruction strategies and innovative transformation pathways.

Depolymerization and fractionation of lignin are key steps in its utilization.<sup>8,9</sup> Currently, various chemical, physical, and biological depolymerization methods have been developed.<sup>9</sup> In the industrial application, chemical depolymerization of lignin faces significant challenges, such as high energy consumption,

<sup>a</sup>School of Chemical Engineering and Technology, Tianjin University, Tianjin 300072, China. E-mail: bzli@tju.edu.cn, zhliu@tju.edu.cn

<sup>b</sup>State Key Laboratory of Synthetic Biology and Frontiers Science Center for Synthetic Biology, Tianjin 300072, China

<sup>c</sup>Frontiers Research Institute for Synthetic Biology, Tianjin University, 301799, China

reaggregation tendencies, increased pollution levels, *etc.*<sup>10</sup> Meanwhile, physical methods often serve primarily as auxiliary pretreatment steps to extract lignin suitable for industrial purposes rather than directly degrading lignin itself.<sup>11</sup>

Interestingly, through natural evolution, microorganisms have developed the ability to depolymerize lignin and utilize the aromatic molecules derived from it as carbon sources, establishing a natural pathway for lignin depolymerization. Investigating the enzymes and metabolic pathways of ligninolytic microorganisms has significantly improved the efficiency of lignin biotransformation and utilization.<sup>10,11</sup> The biotransformation of lignin begins with the depolymerization and separation of lignin, followed by the metabolism of oligomers through the “biological funnel” route of aromatic compounds (Fig. 1).<sup>12</sup> The upper pathway serves as a “biological funnel”, converting isomeric substrates into crucial aromatic product intermediates, such as protocatechuic acid and catechol.<sup>12,13</sup> These intermediates undergo further cleavage *via* the aromatic ring cleavage pathway, opening the ring to produce acetyl coenzyme A (CoA) and succinyl CoA. Following the  $\beta$ -ketoadipic acid pathway, these compounds are then inte-

grated into central carbon metabolism.<sup>13</sup> Biological lignin utilization can be conducted under mild conditions and it is often considered environmentally friendly, aligning with global sustainability goals.<sup>14</sup>

However, the full exploitation and utilization of the microbial conversion of lignin have not yet been fully actualized. It is necessary to identify effective ligninolytic enzymes and pathways for lignin depolymerization and conversion.<sup>8,10,14</sup> Recent efforts in lignin utilization have led to the introduction of cutting-edge technologies aimed at addressing these challenges.<sup>15,16</sup> For example, high-throughput screening technologies harness the power of evolution to identify the desired properties of enzymes and strains.<sup>17–19</sup> Laboratory evolution through high-throughput screening can tailor the properties and enhance the performance of targeted ligninolytic strains and enzymes.<sup>20,21</sup> Protein engineering surpasses natural protein libraries for its potential to customize enzyme and strain characteristics.<sup>22</sup> When necessary enzymes for specific target products are absent from metabolic pathways, new enzymes can be created through protein engineering.<sup>23</sup> Additionally, the integration of biological big data with

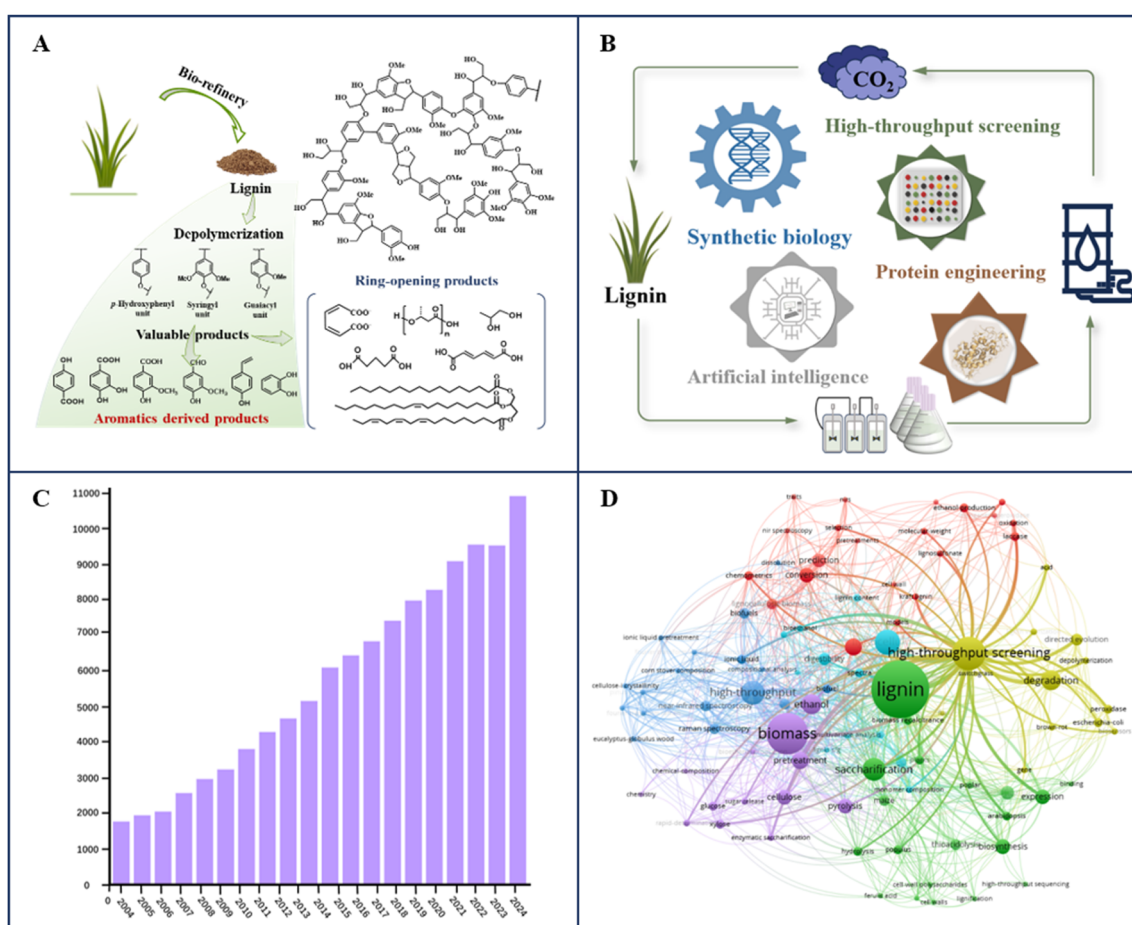


**Fig. 1** The main pathways and research progress of lignin biotransformation. (A) The biological valorization routes from lignin to valuable products. (B) Cutting-edge technologies applied in the progress of lignin biotransformation. (C) Papers published in the field of lignin biotransformation in the past 20 years. (D) Current research work with lignin as the core topic.

bioinformatics tools enables effective analysis and screening.<sup>24–27</sup> Data-driven approaches using artificial intelligence (AI) facilitate advanced strain and enzyme design, guiding directed evolution and reducing experimental iterations.<sup>28–31</sup> Incorporating AI concepts enhances the efficiency of obtaining target strains and enzymes with desired functions and properties.<sup>22,30–33</sup> Overall, these pivotal technologies provide significant opportunities for improving the efficiency of ligninolytic strains and enzymes, thereby advancing the valorization of lignin.

This work aims to advance biological lignin valorization with ligninolytic enzymes by summarizing cutting-edge technologies in the field. First, the biological conversion processes of lignin are reviewed, including macromolecular depolymerization, oligomer degradation, intracellular biological funneling, and ring-opening pathways. Next, advanced technologies for the screening and modification of ligninolytic enzymes are summarized. Powerful tools such as protein engineering and artificial intelligence are highlighted to enable the design and optimization of artificial enzymes with advantages for industrial applications. The cross-application of these multidisciplinary technologies has the potential to drive lignin biological valorization toward a more advanced and intelligent stage of green development.

## 2. Key pathways and enzymes of biological lignin valorization

The microbial valorization of lignin requires a cascade bioconversion route, which mainly includes lignin depolymerization, aromatic metabolism, and product biosynthesis.<sup>22</sup> Preliminary depolymerization of lignin aims to break ether bonds in the structure, resulting in oligomers or monomers for subsequent utilization. This depolymerization generates various heterogeneous lignin-derived aromatic hydrocarbons, which can be further decomposed through the “biological funnel” route. These compounds are metabolized into key intermediates through reactions such as *O*-demethylation, hydroxylation, and decarboxylation.<sup>34</sup> Subsequently, the aromatic intermediates undergo aromatic ring cleavage mediated by dioxygenase. The opened lignin aromatic derivatives then enter the metabolic pathways of microorganisms, such as glycolysis and the tricarboxylic acid cycle, to enable the utilization of lignin-derived aromatic compounds and provide precursors for product biosynthesis.<sup>13</sup>

### 2.1 Depolymerization pathways and enzymes of lignin macromolecules

The initial step of lignin bioconversion involves the depolymerization of lignin by breaking ether bonds to acquire oligomers or monomers for downstream utilization. Various methods exist for the depolymerization of lignin macromolecules, which can be broadly categorized into chemical, biological, physical and physicochemical methods.<sup>8,22</sup>

The structure and properties of natural lignin are influenced by its source and the methods used for fractionation.<sup>34</sup>

Softwood lignin is primarily composed of guaiacyl (G) units and is characterized by a higher molecular weight. Hardwood lignin consists of syringyl (S) and guaiacyl (G) units, with S units being more susceptible to cleavage during acid pretreatment. Herbaceous lignin is primarily composed of G and S units, with a minor contribution from *p*-hydroxyphenyl (H) units.<sup>35,36</sup> In the chemical depolymerization methods of lignin, acid pretreatment is regarded as one of the most effective technologies for cleaving  $\beta$ -O-4 linkages of lignin; however, it leads to lignin’s repolymerization, significantly altering the molecular weight and exhibiting S unit reactivity. Alkaline pretreatment primarily cleaves  $\beta$ -O-4 linkages through nucleophilic cleavage, impacting on the solubility and molecular weight based on alkali concentration and temperature.<sup>37,38</sup> Organosolv pretreatment dissolves lignin in organic solvents, with the molecular weight and structure varying depending on solvent type, temperature, and pretreatment severity.<sup>39,40</sup> This extraction can also be performed using several processes, including organocell, alcell, milox, and ionic liquid lignin extraction.<sup>41</sup> Chemical fractionation methods demonstrated distinct characteristics in modifying lignin chemistry.<sup>42</sup> Chemical depolymerization of lignin also can be performed using methanol, ethanol and peroxyformic acid, as well as various organic cations and inorganic anions (called green solvents).<sup>43</sup> Binary solvent systems consisting of biomass-derived  $\gamma$ -valerolactone and one cosolvent, such as water, ionic liquids, dimethyl sulfoxide and dimethylformamide, were developed as highly efficient systems for the dissolution of various types of lignin.<sup>44</sup> Stirring the sample at 40 and 70 °C induces lignin solubility higher than 200 g kg<sup>-1</sup> and 300 g kg<sup>-1</sup>, respectively. Among various solvent systems,  $\gamma$ -valerolactone/water was the most efficient one. The solubility of lignin could reach 381 g kg<sup>-1</sup> even at 313 K with the content of water being 50 wt%.<sup>44</sup> Although these depolymerization approaches successfully yield aromatic compounds, the bioconversion efficiency of these depolymerized aromatics still requires further evaluation.<sup>45</sup>

Biological depolymerization methods can catalyze the linkages of lignin polymers with powerful ligninolytic enzyme systems. Fungi and bacteria serve as effective ligninolytic microorganisms for lignin depolymerization. Ligninolytic fungi are classified as soft rot fungi, white rot fungi, and brown rot fungi. Ligninolytic bacteria include *Actinobacteria*, *Firmicutes*, *Proteobacteria*, and *Pasteurellales*, encompassing *Actinomyces* such as *Streptomyces* and *Rhodococcus*, as well as *Proteobacteria* such as *Pseudomonas* and *Sphingomonas*.<sup>46</sup> Microorganisms achieve the depolymerization of lignin macromolecules predominantly through their potent oxidase system in lignin-decomposing microorganisms. Ligninolytic enzymes catalyzing lignin depolymerization include laccase, manganese peroxidase, lignin peroxidase, dye-decolorizing peroxidase, glutathione-dependent peroxidase,  $\beta$ -etherases, and auxiliary enzymes that produce hydrogen peroxide (Table 1).<sup>47</sup>

The first type of ligninolytic enzyme in bacteria is laccase, initially characterized in fungi.<sup>47</sup> Bacterial laccase is known to enhance the operational stability of lignin and oxidize a wide range of lignin-derived aromatics.<sup>48</sup> As a multicopper oxidase, it catalyzes the four-proton reduction of O<sub>2</sub> to H<sub>2</sub>O

Table 1 The key enzymes involved in lignin depolymerization for its valorization

Enzymes	Gene sources	Expression strains	Substrates	Enzyme activity	Catalysis reactions	Products	Ref.
Laccase	<i>Trametes villosa</i>	—	SL	—	Redoxidation	H <sub>2</sub>	149
CotA lac	<i>Escherichia coli</i>	—	Lignin phenol derivatives	—	Oxidation	—	150
BL21							
Lac <sup>BL</sup>	<i>Bacillus</i> sp.	<i>E. coli</i> BL21	ABTS, DMP and guaiacol	40.64 IU mg <sup>-1</sup> for ABTS	Depolymerization	Ferulic acid, acetovanillone	151
PCH94							
Lac	Protein Data Bank	—	Lignin polymer, glyphosate, isoproturon and parathion	99.3% degradation for dihydroconiferyl	Detoxification	—	152
			Methylene blue	99.28% decolorization	Decoloration; oxidation	—	153
Lac	<i>Bacillus licheniformis</i>	<i>E. coli</i> BL21	Kraft lignin	—	Oxidation	Lower molecules	154
CotA lac	<i>Bacillus subtilis</i>	<i>E. coli</i>	ABTS	300 U mL <sup>-1</sup>	—	—	155
Lac	<i>Streptomyces coelicolor</i> A3	<i>Pseudomonas putida</i> A514	Maillard products	6.12 U mL <sup>-1</sup> min <sup>-1</sup>	Demethylation	—	156
Manganese peroxidase	SBR	<i>Pseudoduganella violacea</i>	GGE and KL	—	Polymerization	Biphenyl GGE, heptamer length compounds	56
MnP	<i>Ceriporiopsis subvermispora</i>	<i>Pichia pastoris</i> X-33				KL degradation metabolites	157
MnP	<i>B. aryabhattachai</i>	<i>B. aryabhattachai</i>	Kraft lignin	9.2 IU mL <sup>-1</sup>	Demethylation; cleavage of ether linkages; oxidation	—	158
MnP	<i>Phanerochaete chrysosporium</i>	<i>E. coli</i>	Lignin and other phenolic compounds	—	Oxidation	—	159
PcLiP01	<i>P. chrysosporium</i>	<i>P. chrysosporium</i>	LMCs, DHP and MWL	—	C <sub>aryl</sub> –C <sub>α</sub> bond cleavage	DMBQ	159
PcLiPs	<i>P. chrysosporium</i>	<i>E. coli</i> BL21	Melanin		Interrupting π–π stacking and/or hydrogen bonds	—	160
LiP	<i>P. chrysosporium</i>	<i>E. coli</i>	Veratryl alcohol, GGE and VGE	—	Oxidation of nonphenolic aromatics	Dimer phenoxy radicals	161
Dye-decolorizing peroxidase	<i>Bacillus</i> sp. BL5	<i>E. coli</i> BL21	ABTS and alkali lignin	—	Partial oxidation of coniferyl and sinapyl groups of lignin	Low-molecular-weight compounds, vanillin and methoxyphenol	162
PoDyP4	<i>Pleurotus ostreatus</i>	<i>E. coli</i> Rosetta	Zearalenone	9.5 U mg <sup>-1</sup>	Hydroxylation and polymerization	ZEN dimer and four other products	163
CsDyP	<i>Comamonas serinivorans</i>	<i>E. coli</i> BL21	ABTS, GUA, VA, and DMP	317.87 U mg <sup>-1</sup>	Depolymerization and oxidation	Aromatic monomers, low-molecular-weight lignin fractions	164
BsDyP	<i>B. subtilis</i>	<i>E. coli</i> BL21	Lignin model compounds, DMP, guaiacol and VA	—	Oxidation	—	165
DypB	<i>Comamonas testosterone</i>	<i>E. coli</i> BL21	ABTS, DCP and guaiacol	—	Cleavage of C <sub>α</sub> –C <sub>β</sub> linkages	Aldehyde and ketone	58
Versatile peroxidase	<i>Pleurotus eryngii</i>	<i>Pichia pastoris</i>	Rice straw	101 U L <sup>-1</sup> for DMP	Delignification and saccharification	Bioethanol	166
VPs	<i>P. eryngii</i> , <i>P. ostreatus</i>	<i>Saccharomyces cerevisiae</i>	ABTS, DMP, RB5, VA and Mn <sup>2+</sup>	—	Oxidation	—	134
VP	<i>Bjerkandera adusta</i>	—	Lignin from <i>Casuarina equisetifolia</i>	1 U mL <sup>-1</sup> for co-immobilized system	Oxidation of nonphenolic rings	Vanillin	167
VP	<i>Physisporinus</i> sp. strain P18	<i>E. coli</i>	Kraft lignin and natural lignin, dimeric lignin model compounds	19.8 U mg <sup>-1</sup>	Degradation of β-O-4 and 5'-5' types of lignin dimer	Monomeric products	168

SL, *Spartina alterniflora* Loisel; CotA, coating protein A; ABTS, 2,2'-azino-bis(3-ethylbenzothiazoline-6-sulfonic acid); DMP, 2,6-dimethoxy phenol; SBR, Similip Biosphere Reserve; GGE, guaiacylglycerol-β-guaiacyl ether; LMCs, lignin model compounds; DHP, dehydrogenative polymer; MWL, milled wood lignin; DMBQ, 2,6-dimethoxy-1,4-benzoquinone; VGE, veratrylglycerol-β-guaiacyl ether; ZEN, zearalenone; GUA, guaiacol; VA, veratryl alcohol; DCP, 2,4-dichlorophenol; RB5, reactive black 5 (a high-redox potential dye).

accompanied by the one-electron oxidation of four substrate molecules.<sup>49</sup> The depolymerization of lignin by laccase is initiated *via* abstracting a single electron from the phenylpropanoid unit in lignin.<sup>50</sup> Laccase can directly oxidize the phenolic subunits of lignin in the presence of a suitable medium and can also oxidize the non-phenolic units of lignin or high redox potential compounds.<sup>51</sup> The phenolic subunits of lignin are catalyzed to phenoxy radicals by laccase, and the non-phenolic units are oxidized to  $\beta$ -aryl radicals and benzylic radicals by the laccase mediator system.<sup>49</sup> The laccase mediator system can degrade 80–90% of the lignin structure.<sup>52</sup> Peroxidases represent another essential type of ligninolytic enzyme in bacteria, working in conjunction with the co-substrate hydrogen peroxide ( $H_2O_2$ ) to degrade lignin.<sup>53</sup> Based on the type of reaction, peroxidases are classified as manganese peroxidase (MnP), lignin peroxidase (LiP), dye-decolorizing peroxidase (DyP), and versatile peroxidase (VP)<sup>53,54</sup> MnP is a heme-containing glycoprotein and it catalyzes the oxidation of manganese ions ( $Mn^{2+}$ ) to  $Mn^{3+}$  in the presence of  $H_2O_2$ .<sup>55</sup> When using guaiacylglycerol- $\beta$ -guaiacyl ether (GGE) as the substrate, the manganese peroxidase from *Ceriporiopsis subvermispora* (CsMnP) catalyzed the formation of biphenyl GGE linked at the 5–5' position of the phenol ring and generated a heptamer compound.<sup>56</sup> Additionally, CsMnP demonstrated a remarkable ability to polymerize kraft lignin, which increased the molecular weight of the reaction by 360% and significantly reduced the phenol content by 37% in the study using kraft lignin as the substrate.<sup>56</sup> These experiments proved that MnP was an effective biocatalyzer for lignin phenol subunit polymerization. Additionally, the strategy using the enzyme complex of laccase, LiP and MnP was explored to improve the depolymerization efficiency of lignin.

$\beta$ -Esterases have also demonstrated promising potential in the process of lignin degradation.<sup>57</sup> The strains of *Sphingobium*, *Novosphingobium* and other  $\alpha$ -Proteobacteria produce intracellular  $\beta$ -esterases that can utilize glutathione to attack the  $\beta$ -ether bond in lignin fragments.<sup>58</sup> They are also able to cleave lignin dimer compounds through the  $\beta$ -aryl ether degradation pathway to generate vanillin, and then be funneled into the downstream pathway.<sup>59</sup> Therefore, diverse ligninolytic enzymes in bacteria exhibited high substrate specificity, holding the potential to yield suitable lignin-derived aromatics for downstream biotransformation.

Chemical depolymerization methods enable the effective breakdown of lignin, resulting in more versatile aromatic products. However, these methods require high energy inputs and rely on chemical reagents, leading to increased costs.<sup>60</sup> In contrast, biological depolymerization methods, which utilize mild ligninolytic enzyme systems, are more cost-effective and environmentally friendly, offering a viable solution to lignin's challenging degradability.<sup>61</sup> Despite their advantages, biological methods still face challenges related to yield and efficiency, requiring further optimization to achieve more effective depolymerization and support subsequent biotransformation processes. Recently, significant progress has been made in combining chemical and biological depolymer-

ization techniques, demonstrating substantial potential for improving the separation efficiency of lignin components.

## 2.2 Metabolic pathways and enzymes of depolymerized lignin oligomers

After preliminary depolymerization, the depolymerized lignin oligomers can be further metabolized by ligninolytic strains.<sup>62</sup> The lignin-derived oligomers were first catabolized into vanillin and butyric acid, which underwent *O*-demethylation to form catechol derivatives. Catechol derivatives undergo aromatic ring cleavage to produce tricarboxylic acid cycle intermediates.<sup>63</sup> In bacteria, various lignin-derived diaryl and monoaryl groups, along with guaiacyl and syringyl nucleotides, are converted into vanillin and syringic acid through specific ligninolytic enzymes. Vanillin and syringic acid are subsequently demethylated to yield aromatic compounds with catechol structures.<sup>64</sup>

*Sphingomonas* sp. SYK-6 is regarded as an exemplary organism for the decomposition and metabolism of lignin-derived aromatic compounds (Fig. 2).<sup>14</sup> It can absorb various lignin-derived diaryls, such as biphenyls,  $\beta$ -aryl ether, phenylcoumarin, diarylpropane, as well as monoaryls like ferulic acid, vanillin, syringal, and syringal acid.<sup>63</sup> In SYK-6, protocatechusic acid ester 4,5-dioxygenase (LigAB) and gallic acid dioxygenase (DesB) play key roles in the downstream catabolism of lignin derived aromatics with guaiacol and eugenol nuclei, respectively.<sup>65</sup> Due to the abundance of  $\beta$ -aromatic ether bonds in lignin, the study of  $\beta$ -aryl ether cleavage is a vital aspect of lignin degradation. Enzymes involved in  $\beta$ -aryl ether catabolism have been identified, with X-ray crystal structures determined for enzymes such as LigD, LigL, LigF, LigE, LigG, and LigO.<sup>66</sup> The characterized  $\beta$ -aromatic ether catabolism system in bacteria closely resembles that of SYK-6, underscoring the importance of elucidating its role in the natural degradation of  $\beta$ -aromatic ethers.

A bacterial catabolic pathway to phenylcoumarin-type diaryl dehydrodiconiferyl alcohol (DCA) was proposed in *S. paucimobilis* TMY1009 and SYK-6.<sup>63</sup> In the catabolic pathway to dehydrodiconiferyl alcohol identified in SYK-6, the alcohol group of the B-ring side chain of dehydrodiconiferyl alcohol was first oxidized to a carboxyl group and 3-(2-(4-hydroxy-3-methoxyphenyl)-3-(hydroxymethyl)-7-methoxy-2,3-dihydrobenzofuran-5-yl) acrylate (DCA-C) was generated from 3-(2-(4-hydroxy-3-methoxyphenyl)-3-(hydroxymethyl)-7-methoxy-2,3-dihydrobenzofuran-5-yl) acrylaldehyde (DCA-L). The alcohol group of the A-ring side chain of DCA-C was converted into 5-(2-carboxyvinyl)-2-(4-hydroxy-3-methoxyphenyl)-7-methoxy-2,3-dihydrobenzofuran-3-carboxylate (DCA-CC) by two-step oxidation. The C<sub>γ</sub>-carboxyl group of the A-ring side chain of DCA-CC was decarboxylated to produce 3-(4-hydroxy-3-(4-hydroxy-3-methoxystyryl)-5-methoxyphenyl)acrylate (DCA-S), which was further cleaved between C<sub>α</sub> and C<sub>β</sub> of the A-ring side linkage to form vanillin and 5-formylferulate. Finally, ferulic acid was prepared by removing the formyl group of 5-formyl-ferulic acid.<sup>63</sup> In this metabolic pathway, multiple quinone protein alcohols and aryl alcohol dehydrogenases in SYK-6 par-

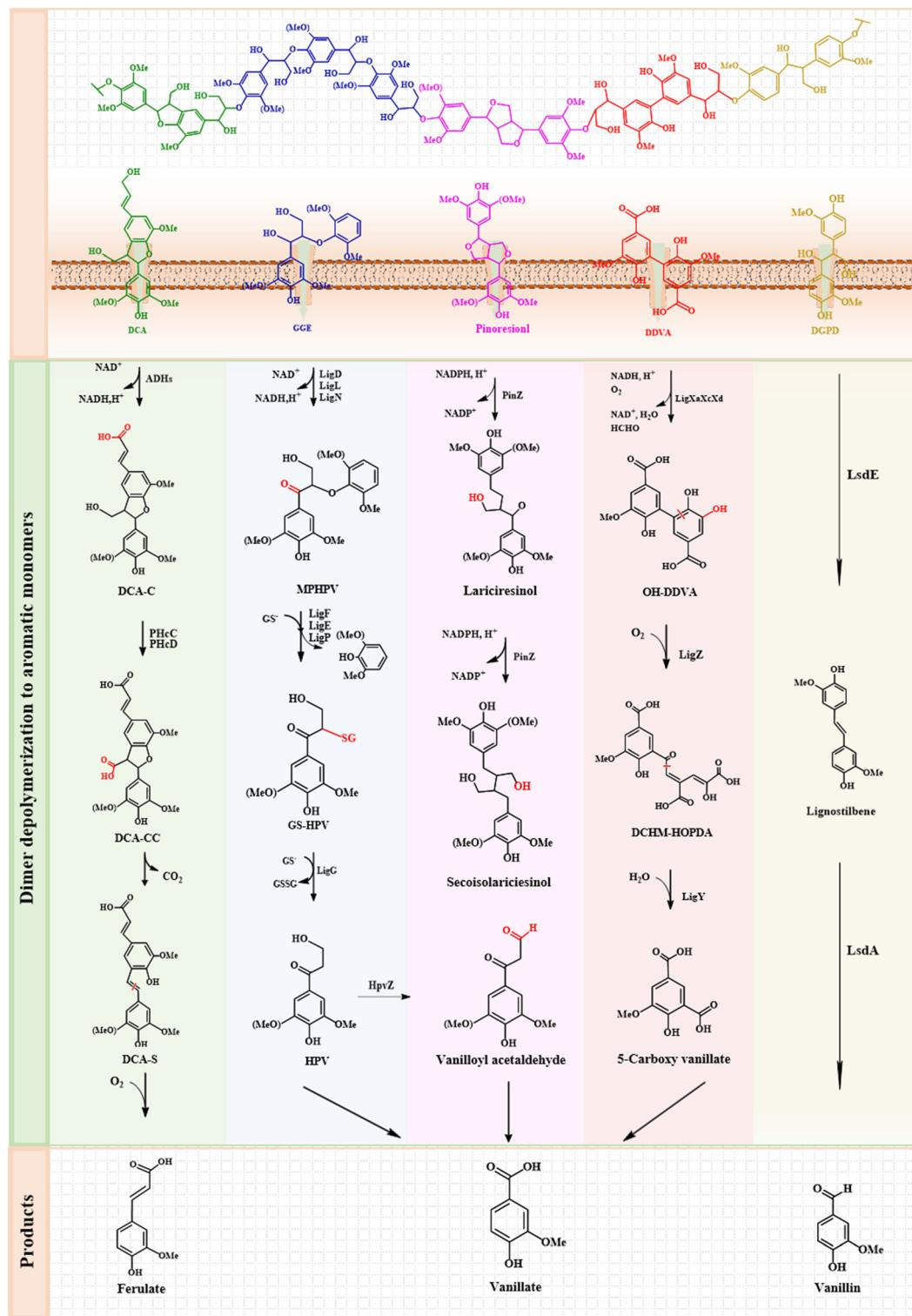


**Fig. 2** Main catabolic pathways of lignin-derived compounds. The lignin polymer model is shown at the top. Lignin polymer is initially depolymerized into oligomers and transported across the membrane into the cell, the oligomer compounds with guaiacyl and syringyl nuclei are then funnelled into vanillate and syringate, respectively. DCA, dehydrodiconiferyl alcohol; GGE, guaiacylglycerol- $\beta$ -guaiacyl ether; DDVA, 5,5'-dehydروdivanillate; DCA-C, 3-(2-(4-hydroxy-3-methoxyphenyl)-3-(hydroxymethyl)-7-methoxy-2,3-dihydrobenzofuran-5-yl)acrylate; DCA-CC, 5-(2-carboxyvinyl)-2-(4-hydroxy-3-methoxyphenyl)-7-methoxy-2,3-dihydrobenzofuran-3-carboxylate; DCA-S, 3-(4-hydroxy-3-(4-hydroxy-3-methoxystyryl)-5-methoxyphenyl)acrylate; MPHVP,  $\alpha$ -(2-methoxyphenoxy)- $\beta$ -hydroxypropiovanillone; GS-HPV,  $\alpha$ -glutathionyl- $\beta$ -hydroxypropiovanillone; HPV,  $\beta$ -hydroxypropiovanillone; OH-DDVA, 2,2',3-trihydroxy-3'-methoxy-5,5'-dicarboxybiphenyl; DCHM-HOPDA, 4,11-dicarboxy-8-hydroxy-9-methoxy-2-hydroxy-6-oxo-6-phenylhexa-2,4-dienoate.

ticipate as dehydrodiconiferyl alcohol convertases. Aryl alcohol dehydrogenases play a major role in the oxidation of dehydrodiconiferyl alcohol, while aldehyde dehydrogenases participate in the transformation of DCA-L.<sup>67</sup> Cytoplasmic and membrane-located SLG\_09480 (*phcC*) and SLG\_09500 (*phcD*) act as enantioselective oxidases responsible for the oxidation of C<sub>γ</sub> alcohols in the A-ring side chain of DCA-C.<sup>68</sup> Additionally, the guaiacylglycerol-β-guaiacyl ether oxidoreductase family in SYK-6 plays an important role in the oxidation of alcohols at C<sub>γ</sub> of C<sub>6</sub>-C<sub>3</sub> lignin-derived compounds.<sup>68</sup>

The β-β bond typically represents secondary linkages that need to be metabolized in other lignin-derived diaryl groups. Pinol and syringoresinol are typical β-β dimers, also known as lignans. (±)-Pinoresinol cannot be utilized as the only carbon source and energy material by SYK-6, whereas (±)-secoisolariciresinol can be produced through the two-step reductive ether cleavage of (±)-lariciresinol.<sup>69</sup> The presence of the *pinZ* gene in SYK-6 is crucial, as the atypical short-chain dehydrogenase/reductase encoded by this gene enables the transformation of (±)-pinoresinol. This enzyme also exhibited activity against syringoresinol. Therefore, the accumulation of the secondary isoleucine glucoside in *pinZ* transgenic plants can be achieved by reducing the levels of abiesterol and its glucoside.<sup>67</sup> As another secondary component of lignin, the β-1 structure mainly exists in the form of a spirodienone structure.<sup>70</sup> *S. paucimobilis* TMY1009 can degrade a β-1 compound such as 1,2-bis(4-hydroxy-3-methoxyphehyl)-1,3-propanediol (HMPPD). 1,2-Bis(4-hydroxy-3-methoxyphehyl)-1,3-propanediol initially underwent C<sub>γ</sub> deformylation while dehydroxylation at C<sub>α</sub> produced a stilbene-type compound. TMY1009 possessed four lignostilbene α,β-dioxygenase (LSD) isoenzymes to convert β-1 lignin stilbenes into two equivalents of vanillin. However, the actual involvement of LSD-I has not been elucidated in the catabolism of 1,2-bis(4-hydroxy-3-methoxyphehyl)-1,3-propanediol.

Overall, lignin-derived oligomers undergo further assimilation under the catalysis of various enzymes. This process not only reveals the potential biological conversion pathways for lignin but also lays the foundation for the subsequent development of "biological funnel" pathways. This step is a crucial component in the conversion of lignin into high-value products. At the same time, continuing to optimize enzyme catalytic efficiency, improve reaction selectivity, and develop new biological conversion pathways remains the key focus of this process.

### 2.3 Biological funnel pathways and enzymes of lignin-derived aromatic monomers

Representative monomers of lignin include *p*-coumaric acid (H-type lignin), ferulic acid (G-type lignin), and syringic acid (S-type lignin). The heterogeneous structure of lignin continues to pose significant challenges, necessitating extensive research efforts to advance its valorization.<sup>71</sup> Some ligninolytic microorganisms such as *Pseudomonas putida* KT2440 have evolved a pathway that converges lignin-derived aromatics into central intermediates, such as protocatechuic acid (PCA).<sup>72</sup>

This metabolic pathway, termed "biological funneling", comprises cascade enzymatic reactions like side-chain cleavage, decarboxylation and oxidation.<sup>72</sup> This strategy enables microbes to funnel diverse aromatic compounds into a single product, preserving the energy stored in the aromatic ring and streamlining lignin metabolism.

The metabolic pathways of H-type aromatics in bacteria can be divided into three categories: coenzyme A (CoA) dependent β-oxidation pathway, coenzyme A dependent non β-oxidation pathway, and coenzyme A independent decarboxylation pathway.<sup>73</sup> The intermediate of *p*-hydroxybenzoic acid was synthesized through these three pathways, and then converted into protocatechuic acid through the 4-hydroxybenzoate-3-monoxygenase PobA. By integrating the beneficial genes for *p*-hydroxybenzoate hydroxylase (PobA) and vanillate O-demethylase oxygenase (VanAB) and implementing the fed-batch strategy, engineered *P. putida* exhibited remarkable PCA production from lignin-derived monomers, achieving a titer of 113.6 mM (17.5 g L<sup>-1</sup>).<sup>74</sup> The metabolic pathways of G-type aromatics in bacteria include coenzyme A-dependent β-oxidation, coenzyme A-dependent non-β-oxidation, non-oxidative decarboxylation and side-chain reduction.<sup>75</sup> These pathways enable the conversion of ferulic acid into vanillic acid intermediates, which are converted into vanillic acid by vanillic acid O-demethylase VanAB. The involvement of class IA oxygenases VanA and VanB reductase in the O-demethylation of vanillin is reported in *Pseudomonas*. A biological funnel pathway was successfully constructed in *S. cerevisiae* by deleting the ADH6, ADH7, BDH2, and FDC1 genes and other optimization strategies.<sup>76</sup> The study successfully obtained protocatechuic acid titers up to 810 mg L<sup>-1</sup> from lignin streams of *p*-coumaric acid and ferulic acid, highlighting that it was a sustainable approach for lignin valorization.

S-Type aromatics possess two methoxy groups in the aromatic ring. Due to a poor demethylation performance in most bacteria, their overall metabolic efficiency remains unsatisfactory.<sup>14</sup> *Sphingomonas* SYK-6 is the best bacterium for the metabolism of S-type aromatics. Degradation through the syringic acid pathway is initiated by tetrahydrofolate dependent O-methyltransferase LigM and DesA, and representative products mainly include protocatechuate, gallic acid and 3-O-methylgallic acid.<sup>77</sup> Heterologous engineering of the O-demethylation system in *P. putida* KT2440 allowed it to metabolize S-type lignin. On this basis, the biosynthesis pathway for *cis,cis*-muconic acid (CCMA) was engineered to simultaneously process three types of lignin-derived aromatics, achieving a remarkable titer and yield of 13.1 mM and 99.5%, respectively.<sup>77</sup>

Other aromatic compounds like phenol, benzene, benzoate, toluene, and naphthalene can be directed to the catechol pathway for further metabolism.<sup>78</sup> Catechol degradation is primarily catalyzed by dioxygenase through *ortho*- or *meta*-cleavage pathways.<sup>76</sup> During the degradation process, catechol 1,2-dioxygenase (catA) and *cis,cis*-muconate cycloisomerase (catB) play important regulatory roles.<sup>79</sup> With the overexpression of catA and inactivation of catB, the engineered strain produced

13.5 g L<sup>-1</sup> *cis,cis*-muconic acid from *p*-CA in a fed-batch bio-reactor.<sup>80</sup> Afterward, further research focused on modifying the metabolically engineered strain *P. putida* KT2440.<sup>81</sup> A synthetic pathway module was designed under the control of the *P<sub>cat</sub>* promoter, comprising both native catechol 1,2-dioxygenases *catA* and *catA2*. This modification aimed to enhance catechol tolerance, increase the levels of catechol 1,2-dioxygenase, and improve catechol conversion rates. The engineered MA-6 strain achieved an *cis,cis*-muconic acid titer of 64.2 g L<sup>-1</sup> from catechol in a fed-batch process.<sup>81</sup>

The biological funnel pathway, along with the associated enzymatic activities, demonstrates the versatility of ligninolytic bacteria in breaking down various lignin-derived aromatic compounds into central intermediates for further metabolism and energy production. Understanding these pathways is crucial for optimizing lignin biotransformation.

#### 2.4 Ring-opening metabolic pathways and enzymes for lignin transformation

Following the biological funnel pathway, key aromatic intermediates further undergo ring-opening pathways to generate various metabolites that can enter central metabolism. Protocatechuiic acid (PCA) follows three distinct ring-opening pathways, namely, the 3,4-cleavage pathway ( $\beta$ -ketoadipic acid pathway), the 4,5-cleavage pathway, and the 2,3-cleavage pathway.

*P. putida* KT2440 harnesses the 3,4-cleavage pathway of protocatechuiic acid catalyzed by protocatechuiic acid 3,4-dioxygenase and a series of enzymes, namely *PcaB*, *PcaC*, *PcaD*, and *PcaI/J*.<sup>12</sup> *Paenibacillus* sp. harnessed the 2,3-cleavage pathway of protocatechuiic acid catalyzed by protocatechuiic acid 2,3-oxygenase, with *PraH*, *PraB*, *PraC*, *PraD* and *PraE*, to yield 4-hydroxy-2-oxyvalerate. The 4,5-cleavage pathway of protocatechuiic acid is found in *Sphingobium* sp. SYK-6 and *Novosphingobium aromaticivorans*, and protocatechuiic acid can be converted into 4-carboxyl-2-hydroxy-mucilate-6-hemialdehyde (CHMS) by protocatechuiic acid 4,5-dioxygenase *LigAB*.<sup>70</sup> 4-Carboxyl-2-hydroxy-mucilate-6-hemialdehyde can be automatically converted into the intramolecular hemiacetal form and then oxidized by 4-carboxyl-2-hydroxy-mucilate-6-hemialdehyde dehydrogenase *LigC* to obtain 2-pyrone-4,6-dicarboxylic acid.<sup>82</sup> 2-Pyrone-4,6-dicarboxylate can be further catalyzed by *LigI/J* to produce 4-carboxyl-4-hydroxy-2-oxadipate (CHA), which is then converted into pyruvate and oxaloacetate under the action of 4-carboxyl-4-hydroxy-2-oxadipate aldolase *LigK*.

Lignin-derived aromatic monomers can be converted into catechol by the catalytic action of protocatechuiic acid decarboxylase. Catechol is then further degraded in bacteria through the *ortho*-cleavage and *meta*-cleavage pathways. *P. putida* KT2440 was engineered to replace the natural protocatechuiic acid 3,4-oxygenase with protocatechuiic acid decarboxylase, enabling the conversion of protocatechuiic acid into catechol.<sup>83</sup> In *Pseudomonas* CF600, the *meso*-cleavage pathway of catechol was initially catalyzed by catechol-2,3-dioxygenase (C2,3D) to produce 2-hydroxymyxohemialdehyde. Additionally, the inter-cleavage pathway of catechol was found in both

Gram-negative and Gram-positive strains.<sup>84</sup> *Sphingomonas* SYK-6 harbored *DesZ* or *LigAB* to catalyze 3-O-methylgallic acid to produce 2-pyrone-4,6-dicarboxylate, which could be integrated into the 4,5-cleavage pathway of protocatechuiic acid and catalyzed by *LigI* to produce 4-oxychloroadone alcohol. Gallic acid was converted into 4-chlorinated salicylic acid by *DesB* or *LigAB*, and then to 4-carboxyl-4-hydroxy-2-oxadipate by *LigI*. 4-Carboxyl-4-hydroxy-2-oxadipate can further be cleaved by *LigK* to form pyruvate and oxaloacetate.

The aforementioned information provides a concise summary of the ring-opening metabolic pathways associated with several key intermediates derived from lignin. It is important to note that different ligninolytic strains may exhibit distinct catabolic preferences for aromatic compounds, reflecting their unique enzymatic machinery and metabolic adaptations. These variations highlight the need for strain-specific optimization to maximize lignin valorization efficiency.

In conclusion, exploring and identifying more comprehensive and potent biocatalytic systems within microorganisms is crucial for advancing lignin utilization. Recent advances in multi-omics approaches have enabled the discovery of novel enzymes and pathways, which expand the toolbox for lignin depolymerization and bioconversion (Table 2). Additionally, the application of synthetic biology and protein engineering techniques enables the design of tailored microbial strains with enhanced lignin-degrading capabilities. Furthermore, understanding the regulatory mechanisms governing aromatic catabolism in ligninolytic microbes can provide valuable insights into improving their performance under industrial conditions. For instance, elucidating the role of transcriptional regulators and stress response systems in these organisms could lead to the development of more robust biocatalysts capable of withstanding inhibitory compounds and harsh processing environments. Therefore, the exploration of microbial biocatalytic systems could not only deepen our understanding of lignin metabolism but also pave the way for more efficient and sustainable lignin valorization.

### 3. High-throughput screening identified ligninolytic enzymes and strains

#### 3.1 Fluorescence-activated cell sorting (FACS) for ligninolytic enzymes

Fluorescence-activated cell sorting (FACS) is a sorting type of flow cytometry that enables the simultaneous analysis of multiple parameters of single cells from a mixed population and the rapid sorting of target cells (Fig. 3).<sup>85</sup> FACS, which relies on fluorescence as a signal source, is the most widely used screening strategy. This method can be further classified based on the type of fluorescence used, including fluorescent substrates, fluorescent proteins, and DNA fluorescent probes. Fluorescent substrates, in particular, are commonly employed in enzyme engineering, as enzymes can cleave these substrates, releasing

Table 2 Summary of recent technological advances in ligninolytic enzymes

Screening methods	Evolution methods/ library design	Library size	Expression strains	Enzymes	Detection substrates	Outcomes	Ref.
Two-step high-throughput screening	—	—	82 bacterial and 46 fungal strains	Laccases	2,6-DMP	Identified ten bacterial and five fungal strains with high laccase activities and the highest laccase activity achieved 133.44 U L <sup>-1</sup>	94
InVitroFlow technology platform	Multisite saturation mutagenesis	3.6 × 10 <sup>6</sup>	<i>Escherichia coli</i> BL21	CelA2 cellulase	4-MUC	The cellulase variant CelA2-M3 showed an 8-fold increase in activity and a 41-fold increase in activity against 4-MUC	98
High-throughput colorimetric assay	Directed and focused molecular evolution	11 500	<i>Saccharomyces cerevisiae</i>	Laccases	Catechol and 2,5-DABSA	The laccase mutant was secreted at 37 mg L <sup>-1</sup> , and its catalytic efficiency for catechol and 2,5-DABSA was improved by 3.5 times	99
Droplet-based microfluidic platform based on a cellulase-catalyzed reaction	Atmospheric and room temperature plasma (ARTP) mutagenesis	—	<i>Pichia pastoris</i>	Heterogeneous cellulase	FCB	The cellulase mutant showed a 7-fold increase in enzyme activity to 11 110 U mL <sup>-1</sup>	106
Diverse functional profile screening experiments	PROSS stability design calculations	43	Yeast	Versatile peroxidases	ABTS	The activities of the two versatile peroxidase mutants were increased 11-fold and 14-fold, respectively	122
Measured $v_i$ , $K_D$ and $k_{cat}$ , $K_m$ parameters	Structure-guided protein engineering and molecular dynamics	—	<i>P. putida</i> KT2440	GcoAB enzyme system	O- and p-vanillin	Demonstrated GcoAB and its single amino acid variants could catalyze a wide range of aromatic O-demethylations	126
High-throughput screening monitored for ABTS and DMP oxidation in 96-well plates	Three rounds of mutagenesis by error-prone PCR	6000	<i>E. coli</i>	Dyp	H <sub>2</sub> O <sub>2</sub> , ABTS and 2,6-DMP	The Dyp variant 6E10 achieved 100-fold increase in catalytic efficiency for 2,6-DMP, and it also demonstrated resistance to hydrogen peroxide inactivation and was produced in 2-fold higher yields	130
The libraries were screened for activity towards DCP and alkali Kraft lignin SEM and XRD monitored the changes of rice straw	Combinatorial active site saturation (CAST) method	546	<i>Pseudomonas fluorescens</i> Pf-5	Dyp1B	DCP and alkali Kraft lignin	The H169L mutant showed an eightfold increase in catalytic efficiency	119
	Artificial intelligence modeling and molecular docking verification	1000	<i>C. testosteroni</i> FJ17	Laccases	Rice straw	The degumming mechanisms of laccase and lignin compounds were revealed and the laccase activity reached 2016.7 U L <sup>-1</sup>	143
Statistical analysis by RSM	Experimental modeling through the ANN-GA	135	<i>Pleurotus sajor-caju</i>	Laccase and MnP	Pulp wash (PW)	Laccase and manganese peroxidase could decolorize the dye up to 89.4% and 75%, respectively	144

2,6-DMP, 2,6-dimethoxy phenol; 4-MUC, 4-methylumbelliferyl- $\beta$ -D-cellobioside; 2,5-DABSA, 2,5-diaminobenzenesulfonic acid; FCB, fluorescein di- $\beta$ -D-cellobioside; ARTP, atmospheric and room temperature plasma; ABTS, 2,2'-azino-bis(3-ethylbenzothiazoline-6-sulfonic acid);  $v_i$ , initial reaction rates;  $K_D$ , equilibrium dissociation constants;  $k_{cat}$ ,  $K_m$ , apparent steady-state kinetics; GcoAB enzyme system, a new architectural class of P450 with a cytochrome P450 monooxygenase (GcoA) and a three domain reductase (GcoB); DCP, 2,4-dichlorophenol; SEM, scanning electron microscopy; XRD, X-ray diffraction; RSM, response surface methodology; ANN-GA, artificial neural networks technique coupled to the genetic algorithm.

fluorescent products. Common fluorescent substrates include catechol, coumarin, fluorescein, and resorufin.<sup>86,87</sup> The core of this technology is the coupling of genotype and phenotype, with the key being the conversion of phenotypic signals into detectable indicators for large-scale screening.<sup>88,89</sup>

Lignin contains various conjugated structural units that emit a bluish-green glow when exposed to ultraviolet light,

making it a key contributor to the fluorescence observed in plant cell walls.<sup>90</sup> Lignin exhibited a peak fluorescence at approximately 400 nm, and demonstrated a broad emission spectrum that extends from the near-ultraviolet to the entire range of visible light wavelengths. However, the exact fluorophoric elements responsible for lignin's fluorescence are still not fully understood. Its fluorescent characteristics, neverthe-

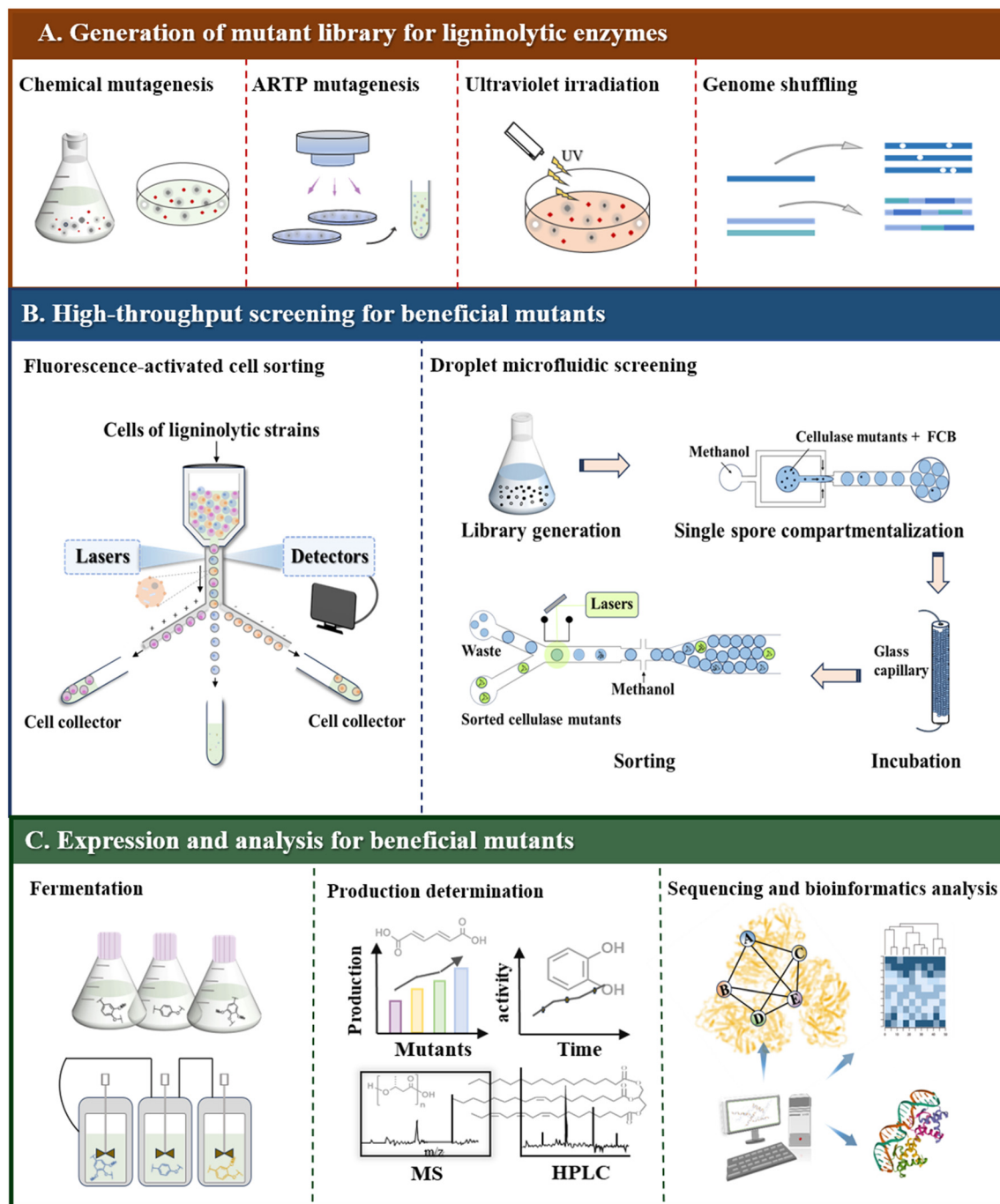


Fig. 3 The workflow for high-throughput screening identified ligninolytic enzymes and strains. FCB, fluorescein di- $\beta$ -D-cellobioside.

less, resemble those of certain model compounds, particularly those with anionic, stilbene, and phenylcoumarone structures, including pinol.<sup>90,91</sup> The variation in emission wavelengths of lignin's fluorescence can be attributed to the combined effects of clustering and the spatial conjugation of its phenylpropane components and benzene rings, at shorter and longer wavelengths, respectively. These characteristics of lignin enabled the synthesis and application of lignin-based fluorescence resonance energy transfer pH fluorescent probes. A significant

technology for determining lignin content emerged by correlating its concentration with the level of fluorescence. Nevertheless, lignin's photoluminescent properties in solution can be influenced by various types of aggregation, including the dimming of fluorescence due to aggregation and the enhancement of brightness due to luminescent aggregation.<sup>92</sup> Similarly, the complex and heterogeneous macromolecular structure of lignin complicates the design of fluorescent substrates. Environmental factors such as solution concentration,

temperature, solvent polarity, pH, viscosity, ion type, ionic strength, and pressure also significantly affect lignin's fluorescence behavior. Bridging this knowledge gap is essential for advancing the use of lignin as a fluorescence tool in high-throughput screening technologies.

High-throughput screening technologies enable the rapid isolation of new ligninolytic microorganisms from a large number of natural biomasses.<sup>93</sup> Advanced technologies in microbiological culture enrichment and enzyme-activity-based screening facilitated a comprehensive study conducted on decaying wood samples collected from the Ottawa region in Canada.<sup>94</sup> A total of 50 samples were meticulously collected and subjected to a battery of tests to identify and isolate microorganisms pivotal in the decomposition process. This rigorous scientific inquiry successfully led to the isolation of a diverse microbial population, comprising 82 distinct bacterial strains and 46 unique fungal strains.<sup>94</sup> The isolation of such a high number of strains underscored the richness of microbial diversity in decaying wood ecosystems and provided a valuable resource for further ecological and applied research. This methodology established a new standard for the isolation of microorganisms from natural environments, especially those involved in the degradation of lignocellulosic biomass. Additionally, a heat- and alkali-tolerant enterobacterium was isolated from sediment samples collected at the mouth of the Mandovi River on the west coast of India.<sup>95</sup> The strain was identified as a highly efficient producer of xylanase, along with ligninolytic bacteria and fungi exhibiting high laccase activity. Notably, some of these strains also demonstrated additional enzymatic activities, including xylanase and  $\beta$ -glucanase.<sup>94</sup> This method was applicable not only to screening ligninolytic microorganisms but also to identifying new microbial strains and enzymes from various natural samples, thereby increasing opportunities to isolate desired strains based on specific enzyme activities.<sup>95</sup>

Critical and efficient technologies have been developed for acquiring lignin hydrolase mutants. The combined active site-saturation test (CAST) was sophisticated technology employed to pinpoint critical amino acid residues near an enzyme's active site. This technology leveraged the enzyme's three-dimensional structural data to systematically identify and evaluate the importance of side chain locations crucial for its catalytic function. By saturating the active site with various amino acid substitutions, CAST enabled the determination of the functional significance of individual residues and their interactions within the active site environment. This approach not only enhanced our understanding of enzyme mechanics but also facilitated the rational design of enzymes with enhanced or novel functionalities.<sup>4</sup> The OmniChange mutagenesis method represented a revolutionary tool for site-specific mutagenesis technologies. Unlike traditional methods, OmniChange could simultaneously saturate up to five codons, significantly accelerating the mutagenesis process and enabling a more comprehensive exploration of the sequence space. Moreover, it did not require a minimum distance between target codons, allowing tightly clustered sites to

be mutated in a single experiment. This greatly simplified the process and reduced the time and resources required for repeated mutations.<sup>96</sup> Following the generation of lignin hydrolase mutants, high-throughput screening technologies could be employed to identify mutants with optimal secretion levels, activity, stability, and pH applicability.

Among various high-throughput screening technologies, FACS, which uses cells as detection chambers, has emerged as the preferred choice due to its superior screening efficiency and greater versatility.<sup>97</sup> The most common strategy involved converting non-fluorescent substrates into fluorescent products through enzyme-catalyzed reactions. This approach was typically applied to hydrolases such as cellulase, lipase, and esterase.<sup>11</sup> In this strategy, the substrate must be able to cross the cell membrane or be transported into the cell, where it can generate a fluorescent signal under the catalysis of intracellular enzymes. The InVitroFlow technology screened mutant libraries by first generating them using plasmid DNA templates. Mutant cellulase libraries were then expressed cell-free within water-in-oil (w/o) single emulsions. The activity variations were classified using flow cytometry in water-in-oil-in-water (w/o/w) double emulsions. DNA was subsequently extracted from the (w/o/w) double emulsions, followed by PCR gene amplification, cloning into an expression host, and transformation to express beneficial clones. The plasmid DNA from the best variants was isolated and used as template DNA for the next round of directed evolution and screening.<sup>98</sup> The InVitroFlow method enabled the screening of the multi-site saturated mutagenic library and OmniChange library, targeting four saturated sites at CelA2 cellulase active site. After screening over 36 million events, a significantly improved cellulase variant, CelA2-M3 (H288F/H524Q), was successfully obtained.<sup>86</sup> The specific activity of the cellulase variant reached 83.9 U mg<sup>-1</sup>, which was 8 times higher than that of the wild-type CelA2. Additionally, the specific activity for the substrate 4-methylumbelliferyl- $\beta$ -D-celllobioside was 41 times higher than that of the wild-type CelA2.<sup>98</sup> These results clearly demonstrated the outstanding advantages of the InVitroFlow technology implemented to accelerate screening efforts and revealed the significant potential for improving enzyme activity through natural variation.

Additionally, enzymes such as proteases, which can break special functional bonds, can also be screened using surface display technologies, with yeast commonly used as a display carrier. By combining high-throughput screening technology and directed evolution, a strongly expressed alkaline laccase variant was identified in *Saccharomyces cerevisiae*.<sup>99</sup> This high-throughput screening experiment was based on the oxidative cross-coupling between 2,5-diaminobenzenesulfonic acid (2,5-DABSA) and catechol, catalyzed by laccase at pH 8.0. After the enzyme-catalyzed oxidation reaction, a colorimetric reaction occurs between the originally colorless catechol and 2,5-DABSA. This colorimetric reaction was highly sensitive to pH and could serve as an indicator for evaluating the activity of the laccase variant enzymes. After conducting rigorous benchmark tests on laccase mutants for the oxidation of catechol

and 2,5-DABSA, a mutation library of approximately 1700 mutants was constructed through further evolution. The mutants were then expressed in *S. cerevisiae* and screened using high-throughput colorimetric methods. The final laccase mutant was secreted at 37 mg L<sup>-1</sup>, and its catalytic oxidation efficiency for catechol and 2,5-DABSA at pH 8.0 was improved by 3.5 times compared to the wild type.<sup>99</sup> The resulting laccase mutant was easily secreted, providing a highly significant platform for advancing work related to organic synthesis. Autonomous hypermutation yeast surface display technology (AHEAD) was developed.<sup>21</sup> This synthetic recombinant antibody generation technology mimicked somatic hypermutations in engineered yeast. By applying this screening technology, potent nanobodies targeting SARS-CoV-2 S glycoproteins, G-protein-coupled receptors, and other targets were successfully generated.<sup>21</sup> Additionally, the combination of substrate and fluorescence resonance energy transfer (FRET) probe allowed for the detection of enzyme activity or the screening of active mutants by observing the significant change in substrate fluorescence wavelength before and after the enzyme reaction. A novel cationic probe1 (Mito-H<sub>2</sub>O<sub>2</sub>) targeting mitochondria was sensitive to the presence of H<sub>2</sub>O<sub>2</sub> and could be used to detect H<sub>2</sub>O<sub>2</sub> quickly.<sup>100</sup> The probe featured a fast response time, high specificity, and high sensitivity. This unique organelle targeting fluorescent probe is expected to become a practical tool for H<sub>2</sub>O<sub>2</sub>-related ligninolytic enzymes and to stimulate the production of new organelle specific fluorescent sensor devices.<sup>100</sup>

The sorting method primarily relied on highly sensitive fluorescent probes of hydrogen peroxide. It was also widely applicable to the directed evolution of other flavin adenine dinucleotide-dependent oxidases in *E. coli*. Fungi that transformed lignin in nature did not function well in neutral/alkaline pH ranges and were strongly inactivated at moderate concentrations of OH<sup>-</sup>. Due to the release of organic acids during the metabolism of white rot fungi, lignin decomposition occurred at acidic pH. However, the evolution of oxidation stability in versatile peroxidases can be achieved by designing a high-throughput screening method based on the molar ratio of H<sub>2</sub>O<sub>2</sub> to enzyme. This allowed for the screening of clones with improved activity at alkaline pH while maintaining the activity at acidic pH, thereby altering the pH activity profile of these enzymes. In this way, variants that functioned under both neutral/alkaline and acidic conditions could be obtained, providing significant versatility for various industrial and environmental applications.<sup>101</sup>

As the most promising high-throughput screening method for enzymes, the introduction of FACS technology holds great potential in the field of directed evolution of ligninolytic enzymes. However, practical applications of this screening technology face several challenges. Variability among individual cells and inconsistencies in the transport of target products across cell membranes can lead to a high rate of false positive outcomes during large-scale screenings. To improve FACS technology, it is crucial to align the genotype with phenotype complexities, integrate both internal and external fluo-

rescent signals, and mitigate the effects of erroneous positive results that may skew the information received. Furthermore, FACS technology is limited to detecting fluorescent signals linked with desired lignin derived products inside cells or fluorescent signals of membrane-associated metabolites. Its inability to screen for secreted metabolites and extracellular enzymes in high-producing cells restricts its broader applicability. Therefore, further research is needed to overcome these limitations and advance high-throughput screening instrumentation.

### 3.2 Droplet microfluidic screening of ligninolytic enzymes

Droplet microfluidic screening, a powerful approach for high-throughput screening, relied on a series of complex operations performed on microfluidic chips. These operations included DNA fragment assembly, host cell transformation, cell culture, recombinant protein expression and sophisticated droplet manipulation techniques coupled with ultrafast separation methods.<sup>17</sup> The development of droplet microfluidic screening overcame limitations inherent to traditional liquid-based screening environments.<sup>102</sup> This screening technology was advantageous for enhancing the biosynthesis of chemical substances or improving the properties of extracellular enzymes.<sup>103</sup> It provided robust methodological support for discovering rare cells in bio-directed evolution experiments.<sup>104</sup>

Microfluidic tools for high-throughput functional screening of enzyme libraries have enabled the routine screening of millions of enzyme variants, streamlining the identification of active variants in directed evolution and functional metagenomic projects. A universal high-throughput screening platform for droplet-based microfluidics was proposed and implemented in 2010.<sup>105</sup> Compared to state-of-the-art robotic screening, this system was 1000 times faster, required 10 million times fewer test doses, and offered cost savings estimated to be about 10 million times greater. The system was successfully implemented in directed evolution, leading to the identification of a new mutant of horseradish peroxidase (HRP).<sup>105</sup> Droplet microfluidic screening technology has been reported in enzyme and cell factory engineering. A droplet-based microfluidic high-throughput screening platform was successfully used for whole-cell directed evolution of *P. pastoris* and further improved heterogeneous cellulase production (Fig. 3).<sup>106</sup> The fluorogenic substrate fluorescein di-β-D-cellobioside (FCB) was used to label heterogeneous cellulase, and methanol served as the organic solvent to form fluorescently labeled water-in-oil droplets. After off-chip incubation for cell growth and cellulase expression for 40 h at 30 °C, droplets were analyzed and sorted based on the fluorescence signal, and finally cells were recovered from the sorted droplets. At a sorting rate of 300 droplets per second, the sorting efficiency of the platform reached 94.4%. Finally, after five rounds of iterative atmospheric and room temperature plasma (ARTP) mutagenesis and microfluidic screening, the best mutant strain was obtained, exhibiting cellulase activity of 11 110 U mL<sup>-1</sup>, nearly twofold higher than the starting strain.<sup>106</sup> This high-throughput screening system can also be

applied to engineer other protein-producing filamentous fungi and will provide valuable insights for accelerating whole-cell directed evolution of host strains and enzymes of high industrial interest. A microfluidic screening platform could enhance the efficiency of enzyme kinetics data collection by adjusting the flow rates of the droplets.<sup>107</sup> This method was successfully applied to study the complex dynamics and thermodynamics of engineered haloalkane dehalogenase variants, offering insights into substrate specificity and hydration-related entropy effects. By combining global data analysis with molecular dynamics simulations, this approach guided the design of novel biocatalysts of lignin and provided direction for developing new biocatalysts.<sup>108</sup>

The practical value of high-throughput screening technology using droplet microfluidics is well established. Since the initiation of the Tox21 project, this approach has evaluated approximately 8500 unique chemicals, accumulating a vast repository of over 120 million data points using high-throughput screening technologies.<sup>19</sup> The project's achievements highlighted the transformative power of technological advancements in tackling complex scientific challenges.<sup>19</sup> This strategy was employed for the screening and evolution of ligninolytic enzymes. A genetically programmed vanilla-sensing bacterium was successfully developed and utilized for high-throughput screening of ligninolytic enzyme libraries.<sup>109</sup> Vanilla-sensing bacteria were developed through RNA sequencing analysis, which identified a vanilla-induced promoter. The green fluorescent protein gene was then placed under the control of that promoter. The fluorescence of this biosensing cell was significantly enhanced in the presence of vanillin and could be easily observed using a fluorescence microscope. This biosensor was highly specific to vanillin and could detect vanillin concentrations as low as 200  $\mu$ M.<sup>109</sup> These engineered *E. coli* cells can be used as host cells to screen for enzymes capable of converting lignin into vanillin, thereby significantly enhancing the efficiency of screening ligninolytic enzymes.

Glycosidases, as prominent representatives of industrial hydrolase centers, are extensively used in the degradation of lignocellulosic biomass.<sup>110</sup> A novel screening process was designed with three main steps: liquid droplets, colonies, and lysates, with plasmid transfer to *E. coli* enabling co-encapsulation of single bacteria, lysates, and fluorescent substrates.<sup>111</sup> In a single experiment, absorbance measurements of droplets at multiple adjustable time points were designed, with the flow direction reversed to enable multiple detection of products generated for determining enzyme kinetic parameters.<sup>112</sup> Twelve high-resolution and high-precision datasets of Michaelis-Menten kinetics were obtained, showcasing the substrate's characterization of the glycosidase potential across seven orders of magnitude of  $k_{cat}/K_m$  enzymatic hydrolysis.<sup>113</sup> Glucosidase  $\beta$ -glucuronidase, a member of the glycoside hydrolase 3 family with few homologous enzymes, was successfully identified using the high-throughput screening platform.<sup>111</sup> This system demonstrated high throughput, excellent data quality, and a wide dynamic range, making it suitable for detailed analysis of clones in large-scale combinatorial experiments.

Overall, high-throughput screening based on droplet microfluidics offered various advantages. Each droplet acted as an independent reactor, ensuring mutual independence of the culture environment between cells and minimizing cross-contamination. *In vitro* expression within droplets also reduced the loss of polymorphism and mitigated the toxic effects on host cells. The microfluidic system could process microdroplets at speeds of up to  $10^8$  per day, significantly enhancing the analytical capacity for large-scale samples. Additionally, the small volume of each microparticle, in the picoliter range, drastically reduced reagent consumption, which was particularly advantageous for analyzing expensive samples. However, current droplet microfluidic screening technology has limitations for the identification of ligninolytic enzymes. The entire process relies heavily on manual operation, making it complex and prone to errors. Moreover, issues such as leakage of fluorescent substrates and the need to further improve signal sensitivity and detection range remain for ligninolytic enzymes. Advances in integrating droplet microfluidic screening with new analytical technologies, such as fluorescence resonance energy transfer, fluorescence polarization, mid-infrared spectroscopy, or mass spectrometry, are crucial for enhancing its capabilities. As technology matures and progress is made, droplet microfluidic screening is poised to become a vital tool in synthetic biology and a powerful method for screening bio-banks in directed evolution toward lignin valorization.

## 4. Protein engineering promoted the evolution of ligninolytic enzymes

For biological lignin valorization, it is of great significance to improve the catalysis performance of ligninolytic enzymes.<sup>23</sup> Protein engineering technology enables the transformation of low-yield, promiscuous enzymatic activities into powerful and efficient biocatalysts, providing a promising tool for obtaining ligninolytic enzymes toward lignin valorization.<sup>114,115</sup> Fig. 4 presents the main process of using protein engineering to promote the evolution of ligninolytic enzymes.<sup>116–119</sup>

### 4.1 Protein engineering assists in designing new ligninolytic enzymes

Fungi deploy a suite of powerful oxidoreductase enzymes, with versatile peroxidases standing out due to their robust redox potential.<sup>116</sup> Versatile peroxidases have garnered significant attention in industry due to their capability to break down environmental aromatic pollutants and process lignocellulosic biomass.<sup>117</sup> Despite the promising attributes of versatile peroxidases, producing these enzymes through recombinant technologies poses substantial difficulties. These challenges primarily stem from the necessity to maintain enzyme stability, activity and functionality outside of their native context.<sup>118</sup> So far, the scientific community has successfully characterized the structure of only one versatile peroxidase enzyme in detail.<sup>119</sup> The optimization process aims to enhance the enzyme's expression levels, stability under various conditions,

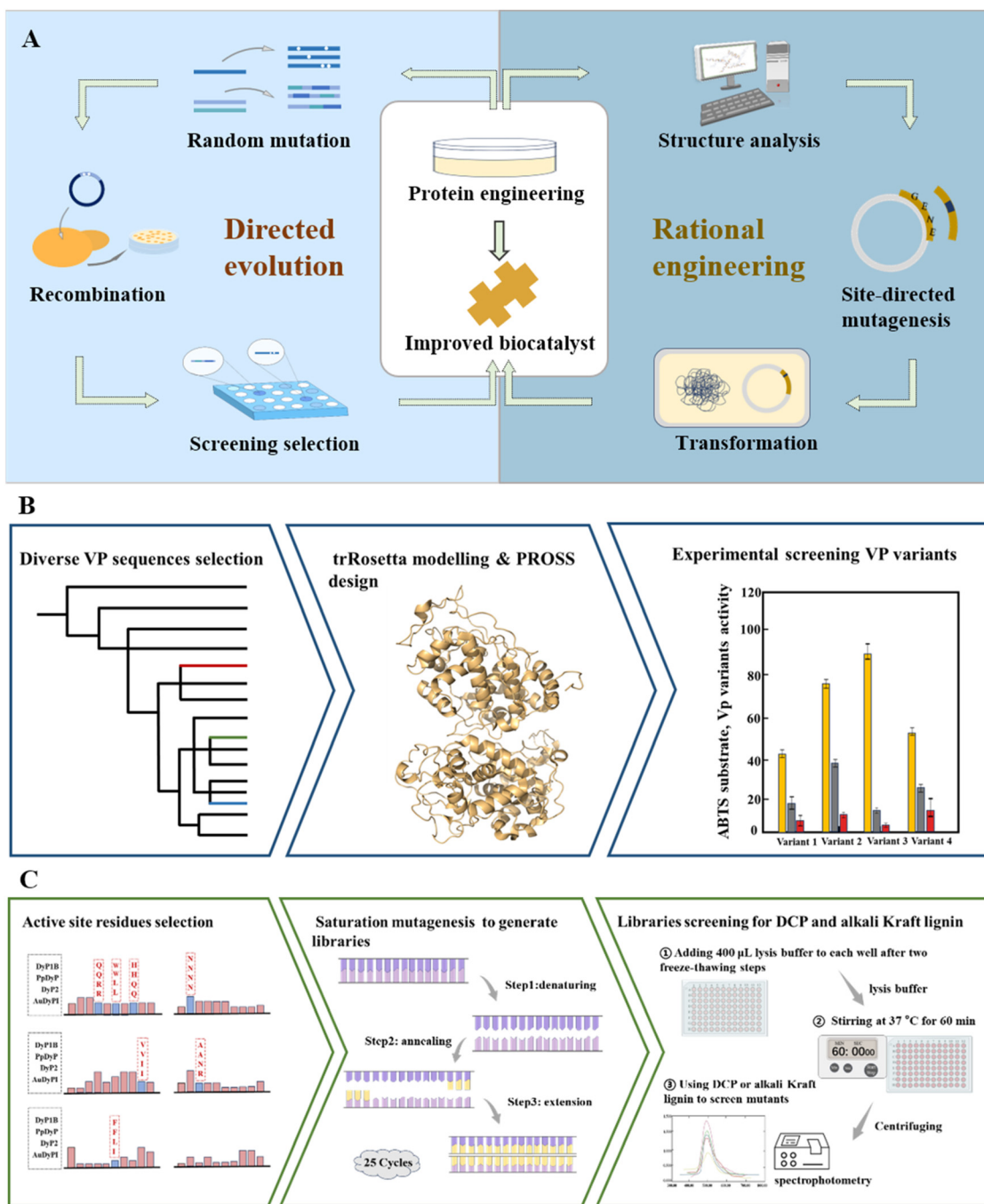


**Fig. 4** Protein engineering promoted the evolution of ligninolytic enzymes. (A) The main protein engineering process to modify ligninolytic enzymes. (B) Key steps in the design of versatile peroxidases with Rosetta modelling and PROSS stability design. (C) The main workflow for using the combinatorial active site saturation (CAST) method to enhance the activity of dye-decolorizing peroxidase Dyp1B enzyme for phenolic and polymeric lignin substrates.

and catalytic activity. This achievement has paved the way for its optimization for recombinant expression, which is essential for practical applications.

A new generation of *ab initio* structure prediction methods based on deep learning have emerged, with the latest methods achieving crystal structure accuracy.<sup>120</sup> The *de novo* deep learning structure prediction method was seamlessly combined

with the PROSS protein stability design strategy to obtain new versatile peroxidases with desired properties (Fig. 4).<sup>121</sup> The stability design of versatile peroxidases was further refined through PROSS to automatically improve the expression and stability of the enzyme, reducing the need for screening thousands of variants.<sup>122</sup> In research, the Rosetta structure prediction algorithm was firstly used to model 11 diverse versatile

peroxidase sequences extracted from public databases and PROSS stability design calculations were run on each sequence.<sup>122</sup> After the design was completed, the versatile peroxidase-encoded sequence was placed downstream of the  $\alpha$  factor leader sequence of the yeast cell and transformed into the yeast cell for functional expression. Based on four diverse versatile peroxidases, a versatile peroxidase from *Pleurotus eryngii* (VPL), two paralogs from *Pleurotus ostreatus* (VP5 and VP11) and a versatile peroxidase from *Ganoderma* sp. 10597\_SS1 (VP8), four functional versatile peroxidases were successfully obtained and denoted as VPLH, 5H, 11H and 8H. The activity of 8H and VPLH increased 11-fold and 14-fold compared to their wild-type enzymes, respectively. Remarkably, the 5H and 11H variants maintained their initial activity levels even after a week of incubation at pH 9. Of all the versatile peroxidase variants, 11H exhibited the highest stability to hydrogen peroxide.<sup>122</sup> The reliability of this new structure prediction and design methodology expanded the scale and scope of computational enzyme optimization for versatile peroxidases, adding significant diversity to the lignin oxidoreductase library characterized to date.

*O*-Aryl-demethylation is an essential step in the aerobic degradation of lignin and its derivatives.<sup>123</sup> *O*-Demethoxylation facilitates the conversion of lignin derivatives into aromatic diols such as catechol, protocatechuic acid and gallic acid. Nearly all lignin-derived aromatics require this crucial step for their conversion into central intermediates.<sup>124</sup> A cytochrome P450 system, GcoAB, was found to demethylate guaiacol (2-methoxyphenol), produced from coniferol-derived lignin, to form catechol.<sup>125</sup> The naturally occurring GcoAB enzyme exhibited limited ability to process syringol (2,6-dimethoxyphenol). Fortunately, the evolution of GcoAB could be achieved through structure-guided protein engineering strategies.<sup>125,126</sup> In the GcoA component of the GcoAB system, the F169 phenylalanine residue was found to obstruct syringol binding. This hindrance arose from a spatial conflict between the side chain of F169 and an additional methoxy group on syringol, which impeded effective binding of eugenol in the active site. Replacing the F169 residue with a smaller amino acid in the mutant GcoA effectively resolved this issue.<sup>125</sup> This substitution mitigated spatial conflict with syringol, allowing syringol to bind more efficiently to the active site of the enzyme. Crystallographic studies and molecular dynamics simulations demonstrated that the mutant GcoA<sup>F169A</sup>, which involved replacing phenylalanine with alanine, performed exceptionally well. Consequently, syringol was efficiently demethylated, and its transformation was successfully achieved in *P. putida* KT2440.<sup>113</sup>

Subsequent studies successfully converted GcoA into a more effective catalyst through single amino acid substitutions.<sup>126</sup> Combining X-ray crystallography and molecular dynamics simulations explained the structural basis for the enhanced activity of the GcoA variant. The active site of GcoA was described as a closely fitting hydrophobic pocket, where a series of hydrophobic amino acids were responsible for positioning the aromatic ring of the substrate. The aromatic ring

of the substrate adopted the planar conformation and relative rotation observed in the wild-type enzyme, thereby providing an optimal presentation of the active methoxy group for the catalysis of the heme. Replacing the smaller alanine residue at position F169 allowed for the binding and demethylation of 2,6-dimethoxyphenol (eugenol). Substituting the primary alcohol (S296) with a secondary alcohol (T296) restored a hydrogen bonding pattern like the wild type around the vanillin aldehyde, enabling a stable binding mode for catalysis. These two amino acid changes reduced spatial conflicts with the aldehyde and provided hydrogen bond donors, making GcoAB an effective catalyst for vanillin isomers. GcoA<sup>F169S</sup> and GcoA<sup>T296S</sup> exhibited strong selectivity for both substrate entry and demethylation of guaiacol or its preferred vanillin isomer.<sup>126</sup> This precise protein engineering not only improved the demethylation efficiency of syringol, but also highlighted the plasticity and potential of the cytochrome P450 system in the biotransformation of lignin-derived aromatics.

Cytochrome P450 systems are among the most versatile enzymes, renowned for their exceptional catalytic versatility.<sup>126</sup> They serve as valuable scaffolds for biotransformation, handling a wide range of substrates and catalyzing numerous chemical reactions.<sup>127</sup> It was demonstrated that the P450 system had an *O*-demethylation effect on guaiacol (2-methoxyphenol).<sup>128</sup> Protein engineering of cytochrome P450 enzymes is evolving into a robust strategy for enhancing the conversion efficiency of lignin components, which is set to improve our understanding of lignin's complex structure and drive the development of innovative transformation technologies.

Overall, the strategic application of protein engineering to design ligninolytic enzymes offered a fresh perspective on harnessing this plentiful resource, potentially redefining the possibilities in lignin valorization and marking a significant step toward more sustainable processing.

#### 4.2 Directed evolution assists in mining new ligninolytic enzymes

Dye-decolorizing peroxidases possess significant potential in lignocellulosic biorefineries due to their ability to oxidize lignin-related compounds.<sup>117</sup> The first bacterial dye-decolorizing peroxidase identified to act on polymeric lignin was dye-decolorizing peroxidase B from *R. jostii* RHA1, a property previously attributed to fungal lignin peroxidase.<sup>129</sup> Bacterial dye-type peroxidases have demonstrated significant potential in converting lignin from industrial processes such as the pulp and paper and the biorefinery industries into value-added products.<sup>130</sup>

Dye-decolorizing peroxidase from *P. putida* MET94 was successfully engineered using error-prone PCR.<sup>130</sup> In the evolution of the *PpDyP* enzyme, a random mutagenesis approach was initially employed to construct a library, and first-generation screening was conducted based on the oxidation capacity of the variants to the substrate 2,2'-azino bis(3-ethylbenzthiazoline-6-sulfonic acid) (ABTS). Then the best-performing variants were selected as the parent for the next round of random mutagenesis. Each generation's screening combined random

mutagenesis and used a color change as a key indicator. Following three rounds of random mutagenesis *via* error-prone PCR on the *PpDyP* gene, the 6E10 variant was subsequently identified through additional high-throughput screening, achieving a remarkable 100-fold increase in catalytic efficiency ( $k_{\text{cat}}/K_m$ ) for 2,6-dimethoxyphenol (DMP). Furthermore, variant 6E10 also demonstrated resistance to hydrogen peroxide inactivation and was produced at 2-fold higher yields.<sup>130</sup> The catalytic efficiency of the evolved variant of dye-decolorizing peroxidase from *P. putida* MET94 was significantly improved on phenolic and aromatic amine substrates in alkaline pH environments. These substrates included Kraft lignin and the model lignin dimer guaiacylglycerol- $\beta$ -guaiacyl, which represented the main chain linkage type in lignin. These results opened numerous opportunities for custom applications utilizing immobilized *PpDyP* variants and studying protein structure within the DyP-type peroxidase family. More importantly, this report was the first to robustly demonstrate the laboratory evolution of bacterial dye-decolorizing peroxidase, highlighting the value of directed evolution in mining new ligninolytic enzymes.

The combinatorial active-site saturation test (CAST) method was developed to obtain effective ligninolytic enzymes.<sup>4</sup> CAST offered an effective alternative to traditional epPCR as the initial step in directed evolution, addressing the long-standing challenge of broad substrate acceptance by enzymes. CAST also enabled the directional evolution of the dye-decolorizing peroxidase Dyp1B from *P. fluorescens* Pf-5 (Fig. 4).<sup>131</sup> A focused library was established at seven active site residues near the heme auxiliary factor relying on saturation mutagenesis, and this library was initially screened using the high redox potential substrate 2,6-dichlorophenol. Then, alkaline Kraft lignin was used for secondary screening, monitoring for increases in absorbance at 465 nm. Analysis of the DyP peroxidase family suggested the presence of residues near the active site and on the protein surface that assisted in catalytic function. Through *in vitro* biotransformation or gene overexpression of ligninolytic strains, the activity of the mutant DyP enzyme on lignin substrate was significantly enhanced. The H169L mutant, which replaced His169 with Leu, exhibited the highest activity for the substrate 2,6-dichlorophenol. The  $k_{\text{cat}}$  value of the H169L mutant was threefold higher than that of wild-type Dyp1B, resulting in an eightfold increase in catalytic efficiency.<sup>131</sup> The discovery offered valuable insights and potential applications for using these more active mutant enzymes to convert lignin into high-value chemicals.

Although the physiological substrate and mechanism of action of dye-decolorizing peroxidases have not yet been clearly defined, these enzymes have garnered increasing attention and study due to their biotechnological potential in lignin valorization. Simultaneously, protein engineering and directed evolution provide promising new approaches for the development of recombinant enzymes and the transformation of lignin substrates. However, engineering robust ligninolytic enzymes remains a challenging task. It is crucial to develop computational modeling and structural analysis in protein

engineering applications to understand the structure–function relationships of ligninolytic enzymes. After elucidating how these enzymes interact with the substrates at the molecular level, it is necessary to design effective mutations that enhance substrate binding, enzyme catalysis, and product release to accelerate the discovery and optimization of ligninolytic enzymes. To further improve the stable ligninolytic enzymes, computational engineering of these enzymes should be explored by building on the success of individual stable mutation designs and incorporating information from several complementary approaches based on evolutionary function or energetic function. Additionally, positive mutant libraries often fail to achieve the desired function due to the prevailing epistasis effect. Addressing these issues is essential for realizing the widespread and efficient application of protein engineering in the high-value conversion of lignin. Overall, protein engineering strategies are crucial for screening ligninolytic enzymes to unlock the potential of lignin as a renewable resource for valuable products.

## 5. Artificial intelligence (AI) boosted the identification of ligninolytic enzymes

Artificial intelligence encompasses the creation of intelligent systems designed to perform tasks that typically require human intelligence, such as learning, problem-solving, and decision-making.<sup>132</sup> AI-driven tools can significantly accelerate the process of ligninolytic enzyme discovery. By integrating data from genomic databases and leveraging predictive models, AI can identify potential ligninolytic enzymes for novel applications without the need for exhaustive laboratory experiments.<sup>133</sup> For instance, machine learning and big data have assisted in ligninolytic enzyme identification and design, thereby enabling sustainable lignin bioconversion toward valuable products.<sup>134</sup>

### 5.1 Artificial intelligence elucidated the mechanism of ligninolytic enzymes

Ligninolytic enzymes exhibit unique molecular and chemical functionalities essential for the comprehensive modification and depolymerization of lignin polymers. These enzymes, pivotal as biocatalysts, boast diverse redox potentials, enabling efficient enzymatic reactions that enhance yields, lower process costs, and mitigate environmental waste.<sup>135</sup> Understanding the intricate mechanisms underlying ligninolytic enzyme action is crucial for advancing lignin valorization.<sup>136,137</sup> Integrating ligninolytic enzymes with artificial intelligence-driven computational frameworks holds promise for potentially achieving breakthroughs to meet escalating industrial demands of ligninolytic enzymes.<sup>31</sup>

Artificial intelligence technology boosts the application of computational frameworks, including docking, molecular dynamics simulation and chemical cracking prediction, in pre-

dicting the bioconversion of lignin.<sup>138–141</sup> A computational framework was employed as the theoretical basis for understanding the degradation mechanism and to enhance the ability to predict ligninolytic enzymes.<sup>142</sup> The Protein Data Bank was utilized to retrieve crystal structures of ligninolytic enzymes including peroxidase, laccase, versatile peroxidase and dye type peroxidase. The ExPasy-ProtParam web server was employed to compute various parameters for each member of the ligninolytic enzyme family. The “SAS-Sequence Annotated by Structure” online server was accessed to predict the sequence annotation of ligninolytic enzymes. A mature modeling tool, CABS-Flex, starting with the CABS input structure, was employed to simulate protein flexibility modeling of ligninolytic enzymes. The final molecular docking between each member of the ligninolytic enzyme families and specific substrates was conducted using AutoDock Vina software (v.1.2.0.). For the final docked complexes, the BIOVIA Discovery Studio Visualizer and PyMOL software were used to capture the binding interactions of the ligand with each ligninolytic enzyme member.<sup>142</sup> The data obtained from the final docking analysis elucidated that versatile peroxidase showed the lowest docking affinity of  $-9.2 \text{ kcal mol}^{-1}$  for the 2,3,7,8-tetrachloro-dibenzo-*p*-dioxin docked complex, indicating that it might effectively catalyze similar pollutants.<sup>142</sup> These results highlighted the binding mode and potential catalysis mechanism of ligninolytic enzymes and further illustrated their potential in the field of ecological environmental remediation.

Artificial intelligence was also successfully employed to elucidate specific functional characteristics of laccases on the bioconversion of lignin-derived compounds. *C. testosteroni* FJ17 employed laccases for the delignification of rice straw (RS), modifying the apparent structure and reduced lignin content in rice straw (Fig. 5).<sup>143</sup> Artificial intelligence modeling and molecular docking revealed the specific functional properties associated with the interaction between laccases and lignin compounds, achieving a peak laccase activity of  $2016.7 \text{ U L}^{-1}$  after 24 h. Scanning electron microscopy and X-ray diffraction analysis confirmed that laccases induced fractures and pores on the surface of rice straw, with crystallinity decreasing from 45.3% to 39.9%, and lignin content decreasing from 19.0% to 10.3%. Gas chromatography-mass spectrometry (GC-MS) and liquid chromatography-mass spectrometry (LC-MS) analysis indicated that the primary delignification mechanism of laccases involved the cleavage of  $\beta$ -O-4 and  $\alpha$ -aryl ether cleavage, resulting in the formation of several small molecular products. The laccase genes were successfully cloned and bioinformatics analysis revealed a sequence comprising 317 amino acids with a predicted molecular weight of 33.13 kDa. Finally, laccase proteins were found to exhibit low binding energies with all tested lignin compounds, and lignin was oxidized by laccases through hydrogen-bonding interactions with the amino acid residues.<sup>143</sup> In conclusion, docking verification, as a reliable method to evaluate the binding affinity between ligninolytic enzymes and substrates, can be used to clarify the mechanism of ligninolytic enzymes and help us predict the theoretical basis of ligninolytic enzymes.

The trained neural network models facilitated the predicted application of lignin-modifying enzymes. The artificial neural network models could optimize the biological decolorization of lignin-modifying enzymes for the azo dye Reactive Black 5 (RB5).<sup>144</sup> Crude RB5 enzyme was obtained from *Pleurotus sajor-caju* as the source of ligninolytic enzymes. An artificial neural network was combined with a genetic algorithm and the response surface method to forecast the decolorization of Reactive Black 5. The results showed that the fungi producing ligninolytic enzymes showed higher laccase activity when growing in pulp washing solution. When immobilized, the fungi showed higher manganese peroxidase activity. Laccase and manganese peroxidase could decolorize the dye up to 89.4% and 75%, respectively.

Overall, artificial intelligence has demonstrated superior performance to tackle the constraints inherent to traditional simulation technologies for ligninolytic enzymes, including issues related to uncertainty, dependence on knowledge-driven models, and substantial computational expenses. To foster a more robust and advanced evolution of artificial intelligence for lignin variolization, there are several areas that warrant ongoing attention and effort. It is crucial to enhance the training of data samples through more extensive case studies of ligninolytic enzymes to evaluate the efficacy of diverse algorithms, and establish more stringent criteria for algorithm selection. It is also necessary to reinforce the processes of data collection, documentation, and sharing within pertinent domains of ligninolytic enzymes. Therefore, the effectiveness of artificial intelligence technologies would be significantly improved, which would guide the identification and engineering of ligninolytic enzymes with the improved accessibility and performance.

## 5.2 Artificial intelligence discovered new ligninolytic enzymes

As biological big data continue to expand, data-driven methodologies leveraging artificial intelligence technologies revolutionize protein and pathway design to tackle the persistent bottleneck in lignin utilization.<sup>28</sup> Enter deep neural networks, which harness amino acid sequence information to forecast the spatial distance between amino acid residues within three-dimensional structures of ligninolytic enzymes. Through rigorous training on a vast array of diverse natural protein structures, deep neural networks have acquired the ability to encode specific protein structural properties. Building upon these advancements, a deep residual network has been devised, enabling the prediction of residue direction and distance swiftly and accurately. This network facilitated the generation of structural models guided by the Rosetta constrained energy minimization protocol, shedding light on the role of each amino acid in determining protein folding sequences. This breakthrough held promise for addressing current hurdles in the *de novo* design of ligninolytic enzyme proteins and was poised to be instrumental in a spectrum of protein structure prediction and design challenges.<sup>145</sup> Furthermore, deep neural networks have been fine-tuned solely on natural

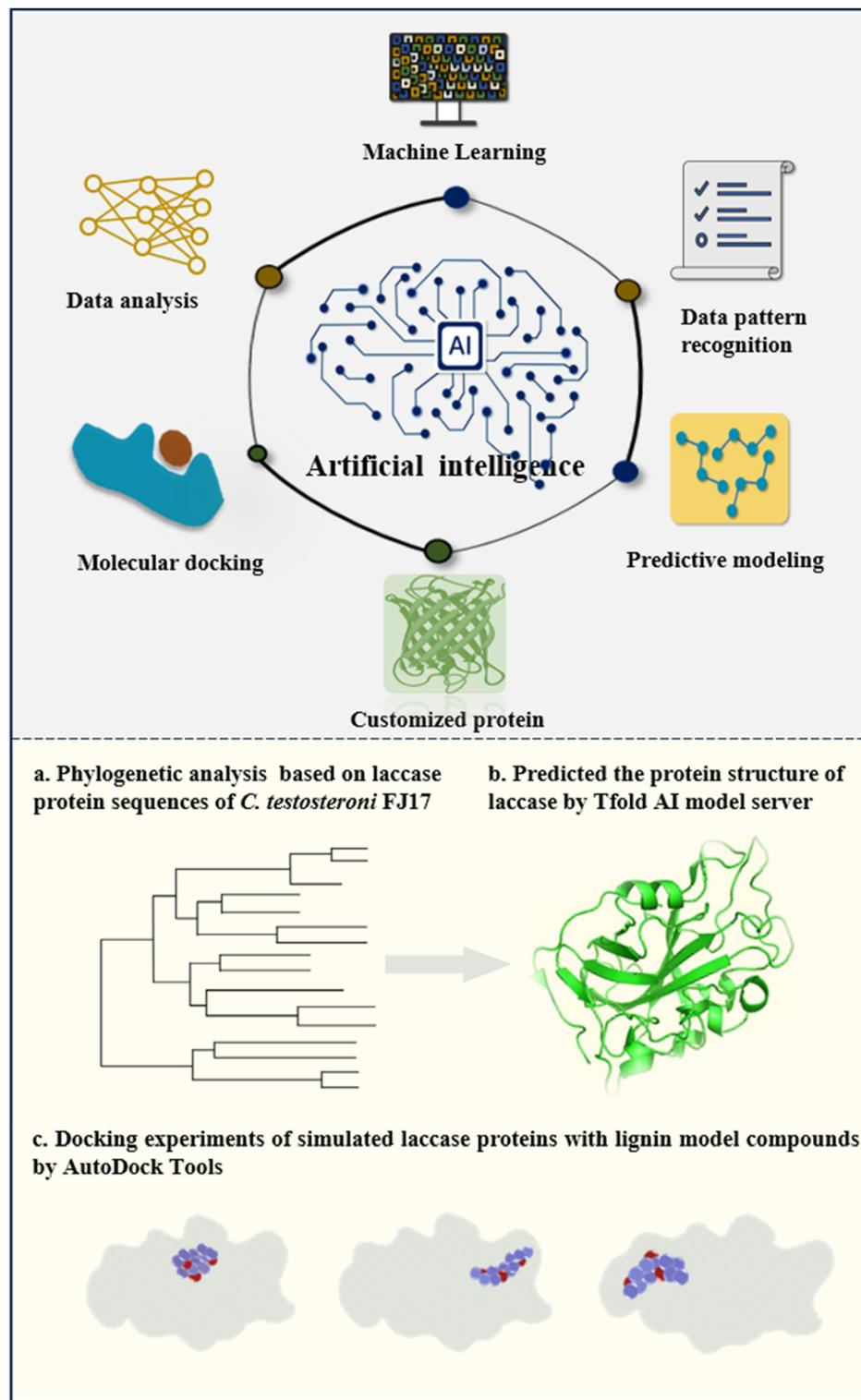


Fig. 5 Artificial intelligence strategies and their applications in designing ligninolytic enzymes.

protein sequences and structures, culminating in the creation of a network capable of generating novel proteins that transcend existing natural sequences, folding into stable structures independently. This innovative approach not only allowed for

the reverse engineering of new ligninolytic enzymes but also complemented traditional physics-based models, ushering in a new era of protein design with enhanced functionalities and capabilities.<sup>146</sup>

Linear discriminant analysis and random forest (RF) machine learning algorithms enabled the elucidation of the complex relationship between genetic information and wood rotting fungi decay patterns. This approach enabled the classification of white rot and brown rot fungi with an accuracy exceeding 98%.<sup>147</sup> The machine learning algorithm primarily relied on the count of carbohydrate active enzyme genes for the differentiation of white rot and brown rot fungi. Within the random forest algorithm, specific genes engaged in cellulose and lignin degradation, such as polysaccharide monooxygenase and cellulose biohydrolase, emerged as pivotal factors in distinguishing between white rot and brown rot fungi.<sup>147</sup> Leveraging algorithms presented a novel avenue for discovering previously unidentified ligninolytic enzymes in nature. These tools not only aided in the categorization of ligninolytic enzymes and microbial strains but also facilitated a deeper exploration of their identities.

The biological degradation of aromatic waste presented a green and sustainable approach. For example, exploring assumed enzyme sequences to unveil new aromatic plastic-degrading enzymes may offer a promising avenue. Enter the plastic enzyme degradation (PED) framework, a cutting-edge development rooted in machine learning technologies. This innovative framework predicted enzyme capabilities in degrading specific aromatic plastics by uncovering latent patterns within protein sequences.<sup>148</sup> It excelled at pinpointing and comprehensively interpreting crucial enzymatic characteristics essential for aromatic plastic degradation. The novel context-aware enzyme sequence representation (CESR) method embedded within the framework excelled at capturing intricate context information within enzyme sequences, extracting enzyme features at both the amino acid and global sequence levels. With an impressive overall accuracy rate of 90.2%, surpassing existing sequence-based protein classification models, the PED framework emerged as a powerful tool for predicting and discovering aromatic plastic-degrading enzymes, paving the way for a more sustainable future.<sup>148</sup>

With the emergence and advancement of artificial intelligence, the integration of computer technology and experimental screening has enhanced the efficiency and intelligence of screening strategies for ligninolytic enzymes and bacteria. The utilization of big data research, driven by the fusion of computer science and artificial intelligence, along with advancements in machine learning, enables the rapid analysis of vast datasets, the identification of patterns, and the provision of accurate results. This significantly aids in the engineering and sustainable development of high-value ligninolytic enzymes. However, it is important to acknowledge that the development of artificial intelligence models poses unique challenges in terms of reproducibility. The widespread adoption of artificial intelligence technology heavily relies on data, necessitating both enough data and high data quality especially for biological lignin valorization. It needs to address the limitations of data quality in the future for achieving the widespread implementation of artificial intelligence.

## 6. Conclusions

Microorganisms have developed the ability to depolymerize lignin and utilize aromatic molecules derived from it as carbon sources, establishing a natural pathway for lignin depolymerization. However, several major challenges remain in the bioconversion of lignin. Biological lignin valorization requires effective depolymerization approaches for lignin and feasible bioconversion routes of lignin-derived aromatics. The efficient depolymerization and bioconversion of lignin have not been fully realized due to the lack of efficient ligninolytic enzymes. The synergistic advancement of synthetic biology alongside other scientific disciplines has paved the way for the discovery of effective ligninolytic enzymes, which serve as promising biocatalysts for depolymerizing and converting lignin into valuable derivatives that engineered microorganisms can further process. Advanced technologies—such as high-throughput screening, protein engineering, and artificial intelligence—could enhance the identification of efficient ligninolytic enzymes, thereby improving the overall efficiency of lignin depolymerization and bioconversion.

First, high-throughput techniques can be employed to screen for efficient biocatalysts with specific functions from a vast array of enzymes or microorganisms. When combined with laboratory evolution, this approach allows for the tailoring of desired biological properties. However, high-throughput screening technologies still face practical challenges. Variability in the levels of single cells and the transport of target products between cells can lead to false positive rates in screenings such as FACS. To effectively screen ligninolytic bacteria and enzymes, it is essential to integrate genotype and phenotype, as well as intracellular and extracellular fluorescent signals, to mitigate misleading information caused by false positives. Second, protein engineering can refine the evolutionary strategies applied to ligninolytic enzymes. This field goes beyond natural protein libraries, aiming to enhance the functionality of modified enzymes with customized properties. This strategy is crucial for overcoming challenges related to missing biological pathways and catalytic inefficiencies. However, efficiently sampling across a broad design space remains a challenge in the quest to design new and more efficient ligninolytic enzyme pathways. Third, data-driven approaches that leverage artificial intelligence technology enable the design of more advanced target strains and enzymes. Integrating AI into the development of ligninolytic strains and enzymes can guide directed evolution, minimizing the number of experimental iterations required to efficiently obtain target strains and enzymes with specific functions and properties. Machine learning-guided directed evolution has proved successful in accelerating optimization cycles and alleviating experimental burdens. It is worth noting that when designing artificial intelligence strategies to assist in the screening and transformation of aromatic polymer degradation enzymes, it is crucial to meet the quantitative requirements of artificial intelligence while ensuring the authenticity and availability of data.

Overall, the integration of the cutting-edge technologies discussed above into lignin high-value research is set to yield groundbreaking advancements. This progress is expected to address the current challenges related to the limited variety and low efficiency of ligninolytic enzymes. However, it is important to recognize that the application of these technologies for lignin valorization is still in the early stages of research and development. Significant efforts remain necessary to achieve the widespread application of these innovative approaches, highlighting the need for continued dedication and progress in this field.

## Data availability

No primary research results, software or code have been included and no new data were generated or analyzed as part of this review.

## Conflicts of interest

The authors declare that they have no competing interests in the article.

## Acknowledgements

This work was supported by the National Key Research and Development Program of China (2023YFC3403500) and the Key Research and Development Program of Ningxia Hui Autonomous Region (2024BEE02005).

## References

- 1 E. T. C. Vogt and B. M. Weckhuysen, *Nature*, 2024, **629**, 295–306.
- 2 M. Zuk, *Science*, 2020, **367**, 1304–1305.
- 3 J. G. Linger, D. R. Vardon, M. T. Guarnieri, E. M. Karp, G. B. Hunsinger, M. A. Franden, C. W. Johnson, G. Chupka, T. J. Strathmann, P. T. Pienkos and G. T. Beckham, *Proc. Natl. Acad. Sci. U. S. A.*, 2014, **111**, 12013–12018.
- 4 R. Y. Liu, Z. H. Liu, B. Z. Li and Y. J. Yuan, *Green Chem.*, 2024, **26**, 11378.
- 5 Z. H. Liu, N. Hao, Y. Y. Wang, C. Dou, F. Lin, R. Shen, R. Bura, D. B. Hodge, B. E. Dale, A. J. Ragauskas, B. Yang and J. S. Yuan, *Nat. Commun.*, 2021, **12**, 3912.
- 6 D. Salvachúa, T. Rydzak, R. Auwae, A. De Capite, B. A. Black, J. T. Bouvier, N. S. Cleveland, J. R. Elmore, A. Furches, J. D. Huenemann, R. Katahira, W. E. Michener, D. J. Peterson, H. Rohrer, D. R. Vardon, G. T. Beckham and A. M. Guss, *Microb. Biotechnol.*, 2019, **13**, 290–298.
- 7 J. R. Elmore, G. N. Dexter, D. Salvachúa, M. O'Brien, D. M. Klingeman, K. Gorday, J. K. Michener, D. J. Peterson, G. T. Beckham and A. M. Guss, *Metab. Eng.*, 2020, **62**, 62–71.
- 8 E. Rosini, F. Molinari, D. Miani and L. Pollegioni, *Catalysts*, 2023, **13**, 555.
- 9 Z. H. Liu, H. Liu, T. Xu, Z. M. Zhao, A. J. Ragauskas, B. Z. Li, J. S. Yuan and Y. J. Yuan, *Renewable Sustainable Energy Rev.*, 2025, **211**, 115296.
- 10 E. Erickson, A. Bleem, E. Kuatsjah, A. Z. Werner, J. L. DuBois, J. E. McGeehan, L. D. Eltis and G. T. Beckham, *Nat. Catal.*, 2022, **5**, 86–98.
- 11 Y. Suzuki, Y. O. Abe, Y. Otsuka, T. Araki, M. Nojiri, N. Kamimura, E. Masai and M. Nakamura, *Bioresour. Technol.*, 2022, **363**, 127836.
- 12 A. Z. Werner, W. T. Cordell, C. W. Lahive, C. A. Singer, B. C. Klein, E. C. D. Tan, M. A. Ingraham and K. J. Ramirez, *Sci. Adv.*, 2023, **9**, eadj0053.
- 13 C. W. Johnson, D. Salvachúa, N. A. Rorrer, B. A. Black, D. R. Vardon, P. C. St. John, N. S. Cleveland, G. Dominick, J. R. Elmore, N. Grundl, P. Khanna, C. R. Martinez, W. E. Michener, D. J. Peterson, K. J. Ramirez, P. Singh, T. A. VanderWall, A. N. Wilson, X. Yi, M. J. Biddy, Y. J. Bomble, A. M. Guss and G. T. Beckham, *Joule*, 2019, **3**, 1523–1537.
- 14 J. Becker and C. Wittmann, *Biotechnol. Adv.*, 2019, **37**, 107360.
- 15 Z. Liu, S. Chen and J. Wu, *Trends Biotechnol.*, 2023, **41**, 1168–1181.
- 16 Y. Liu, H. Yuan, D. Ding, H. Dong, Q. Wang and D. Zhang, *ACS Synth. Biol.*, 2021, **10**, 1373–1383.
- 17 J. Yang, R. Tu, H. Yuan, Q. Wang and L. Zhu, *Crit. Rev. Biotechnol.*, 2021, **41**, 1023–1045.
- 18 S. Chityala, V. Nandana and D. Jayachandran, *Adv. Yeast Biotechnol. Biof. Sustain.*, 2023, pp. 249–275.
- 19 N. Perera and R. S. H. Koralege, *Encyclopedia of Toxicology*, 2023, pp. 297–301.
- 20 M. Yang, Y. Yang, C. Xie, M. Ni, J. Liu, H. Yang, F. Mu and J. Wang, *Nat. Mach. Intell.*, 2022, **4**, 696–709.
- 21 A. Wellner, C. McMahon, M. S. A. Gilman, J. R. Clements, S. Clark, K. M. Nguyen, M. H. Ho, V. J. Hu, J.-E. Shin, J. Feldman, B. M. Hauser, T. M. Caradonna, L. M. Wingler, A. G. Schmidt, D. S. Marks, J. Abraham, A. C. Kruse and C. C. Liu, *Nat. Chem. Biol.*, 2021, **17**, 1057–1064.
- 22 M. Paul, N. K. Pandey, A. Banerjee, G. K. Shrotri, P. Tomer, R. K. Gazara, H. Thatoi, T. Bhaskar, S. Hazra and D. Ghosh, *Bioresour. Technol.*, 2023, **379**, 129045.
- 23 Y. Wang, H. Tang, L. Huang, L. Pan, L. Yang, H. Yang, F. Mu and M. Yang, *Nat. Mach. Intell.*, 2023, **5**, 845–860.
- 24 D. D. Silva and D. Alahakoon, *Patterns*, 2022, **3**, 100489.
- 25 A. Holzinger, K. Keiblinger, P. Holub, K. Zatloukal and H. Müller, *New Biotechnol.*, 2023, **74**, 16–24.
- 26 M. Hutson, *Science*, 2022, **375**, 129–129.
- 27 T. H. Yu, H. Y. Cui, J. C. Li, Y. N. Luo, G. Jiang and H. M. Zhao, *Science*, 2023, **379**, 1358–1363.
- 28 W. D. Jang, G. B. Kim, Y. Kim and S. Y. Lee, *Curr. Opin. Biotechnol.*, 2022, **73**, 101–107.

29 R. L. Sokolik, O. Khersonsky, S. P. Schröder, C. de Boer, S. Y. Hoch and G. J. Davies, *Science*, 2023, **379**, 195–201.

30 N. Konno and W. Iwasaki, *Sci. Adv.*, 2023, **9**, eadc9130.

31 A. K. Singh, H. M. N. Iqbal, N. Cardullo, V. Muccilli, J. Fernández-Lucas, J. E. Schmidt, T. Jesionowski and M. Bilal, *Int. J. Biol. Macromol.*, 2023, **242**, 124968.

32 S. K. Jayasekara, H. D. Jomi, B. Jayantha, L. Dissanayake, C. Mandrell, M. M. S. Sinharage, R. Molitor, T. Jayasekara, P. Sivakumar and L. N. Jayakody, *Comput. Struct. Biotechnol. J.*, 2023, **21**, 3513–3521.

33 I. D. Lutz, S. Z. Wang, C. Norn, A. Courbet, A. J. Borst, Y. T. Zhao, A. Dosey, L. X. Cao, J. W. Xu, E. M. Leaf, C. Treichel, P. Litvicov, Z. Li, A. D. Goodson, P. R. Sánchez, A. M. Bratovianu, M. Baek, N. P. King, H. R. Baker and D. Baker, *Science*, 2023, **380**, 266–273.

34 A. J. Ragauskas, G. T. Beckham, M. J. Biddy, R. Chandra, F. Chen, M. F. Davis, B. H. Davison, R. A. Dixon, P. Gilna, M. Keller, P. Langan, A. K. Naskar, J. N. Saddler, T. J. Tschaplinski, G. A. Tuskan and C. E. Wyman, *Science*, 2014, **344**, 1246843.

35 Z. H. Liu, M. L. Olson, S. Shinde, X. Wang, N. Hao, C. G. Yoo, S. Bhagia, J. R. Dunlap, Y. Pu, K. C. Kao, A. J. Ragauskas, M. Jin and J. S. Yuan, *Green Chem.*, 2017, **19**, 4939–4955.

36 Z. H. Liu, S. Shinde, S. Xie, N. Hao, F. Lin, M. Li, C. G. Yoo, A. J. Ragauskas and J. S. Yuan, *Sustainable Energy Fuels*, 2019, **8**, 2024–2037.

37 J. S. Kim, Y. Y. Lee and T. H. Kim, *Bioresour. Technol.*, 2016, **199**, 42–48.

38 H. Liu, Z. Chen, J. Q. Cui, S. Ntakirutimana, T. Xu, Z. H. Liu, B. Z. Li and Y. J. Yuan, *Ind. Crops Prod.*, 2014, **218**, 118956.

39 N. L. Radhika, S. Sachdeva and M. Kumar, *Fuel*, 2022, **312**, 122935.

40 N. Zhou, W. P. D. W. Thilakarathna, Q. S. He and H. P. V. Rupasinghe, *Front. Energy Res.*, 2022, **9**, 758744.

41 J. G. Linger, D. R. Vardon, M. T. Guarnieri, E. M. Karp, G. B. Hunsinger, M. A. Franden, C. W. Johnson, G. Chupka, T. J. Strathmann, P. T. Pienkos and G. T. Beckham, *Proc. Natl. Acad. Sci. U. S. A.*, 2014, **111**, 12013–12018.

42 A. Tribot, G. Amer, M. Abdou Alio, H. de Baynast, C. Delattre, A. Pons, J. D. Mathias, J. M. Callois, C. Vial, P. Michaud and C. G. Dussap, *Eur. Polym. J.*, 2019, **112**, 228–240.

43 N. Muhammad, Z. Man and M. A. Bustam Khalil, *Eur. J. Wood Wood Prod.*, 2011, **70**, 125–133.

44 Z. Xue, X. Zhao, R. C. Sun and T. Mu, *ACS Sustainable Chem. Eng.*, 2016, **4**, 3864–3870.

45 C. Mukesh, G. Huang, H. Qin, Y. Liu and X. Y. Ji, *Biomass Bioenergy*, 2024, **188**, 107305.

46 D. P. Brink, K. Ravi, G. Lidén and M. F. G. Grauslund, *Appl. Microbiol. Biotechnol.*, 2019, **103**, 3979–4002.

47 G. W. Park, G. Gong, J. C. Joo, J. Song, J. Lee, J. P. Lee, H. T. Kim, M. H. Ryu, R. Sirohi, X. Zhuang and K. Min, *Renewable Sustainable Energy Rev.*, 2022, **157**, 112025.

48 S. T. Zhang, Z. J. Dong, J. Shi, C. R. Yang, Y. Fang, G. Chen, H. Chen and C. J. Tian, *Bioresour. Technol.*, 2022, **361**, 127699.

49 M. Zhou, O. A. Fakayode, M. Ren, H. X. Li, J. K. Liang, A. E. A. Yagoub, Z. Fan and C. S. Zhou, *Bioresour. Bioprocess.*, 2023, **10**, 21.

50 M. Zhou, L. Z. Tao, P. Russell, R. D. Britt, T. Kasuga, X. Lü and Z. L. Fan, *Ind. Crops Prod.*, 2022, **188**, 115650.

51 Z. Li, J. Zhang, L. Qin and Y. Ge, *ACS Sustainable Chem. Eng.*, 2018, **6**, 2591–2595.

52 C. Chio, M. Sain and W. Qin, *Renewable Sustainable Energy Rev.*, 2019, **107**, 232–249.

53 O. D. V. Biko, M. V. Bloom and W. H. V. Zyl, *Enzyme Microb. Technol.*, 2020, **141**, 109669.

54 A. O. Falade, U. U. Nwodo, B. C. Iweriebor, E. Green, L. V. Mabinya and A. I. Okoh, *Wiley Interdiscip. Rev.: Comput. Mol. Sci.*, 2017, **6**, e00394.

55 A. Kumar and P. K. Arora, *Front. Environ. Sci.*, 2022, **10**, 875157.

56 K. S. K. Teo, K. Kondo, T. Watanabe, T. Nagata and M. Katahira, *ACS Sustainable Chem. Eng.*, 2024, **12**, 2172–2182.

57 J. M. Guo, D. Liuc and Y. Xu, *Sustainable Energy Fuels*, 2024, **8**, 1153–1184.

58 G. M. M. Rashid and T. D. H. Bugg, *Catal. Sci. Technol.*, 2021, **11**, 3568–3577.

59 P. D. Sainsbury, E. M. Hardiman, M. Ahmad, H. Otani, N. Seghezzi, L. D. Eltis and T. D. H. Bugg, *ACS Chem. Biol.*, 2013, **8**, 2151–2156.

60 N. L. Radhika, S. Sachdeva and M. Kumar, *Fuel*, 2022, **312**, 122935.

61 Z. Chen and C. Wan, *Renewable Sustainable Energy Rev.*, 2017, **73**, 610–621.

62 E. Masai, Y. Katayama and M. Fukuda, *Biosci. Biotechnol. Biochem.*, 2007, **71**, 1–15.

63 N. Kamimura, K. Takahashi, K. Mori, T. Araki, M. Fujita, Y. Higuchi and E. Masai, *Environ. Microbiol. Rep.*, 2017, **9**, 679–705.

64 R. Y. Liu, H. N. Lan, Z. H. Liu, B. Z. Li and Y. J. Yuan, *Renewable Sustainable Energy Rev.*, 2024, **191**, 114205.

65 K. Mori, N. Kamimura and E. Masai, *Appl. Microbiol. Biotechnol.*, 2018, **102**, 4807–4816.

66 J. H. Pereira, R. A. Heins, D. L. Gall, R. P. McAndrew, K. Deng, K. C. Holland, T. J. Donohue, D. R. Noguera, B. A. Simmons, K. L. Sale, J. Ralph and P. D. Adams, *J. Biol. Chem.*, 2016, **291**, 10228–10238.

67 M. Tamura, Y. Tsuji, T. Kusunose, A. Okazawa, N. Kamimura, T. Mori, R. Nakabayashi, S. Hishiyama, Y. Fukuhara, H. Hara, K. Sato-Izawa, T. Muranaka, K. Saito, Y. Katayama, M. Fukuda, E. Masai and S. Kajita, *Appl. Microbiol. Biotechnol.*, 2014, **98**, 8165–8177.

68 L. Kirmair and A. Skerra, *Appl. Environ. Microbiol.*, 2014, **80**, 2468–2477.

69 Y. Fukuhara, N. Kamimura, M. Nakajima, S. Hishiyama, H. Hara, D. Kasai, Y. Tsuji, S. Narita-Yamada, S. Nakamura, Y. Katano, N. Fujita, Y. Katayama,

M. Fukuda, S. Kajita and E. Masai, *Enzyme Microb. Technol.*, 2013, **52**, 38–43.

70 Y. Matsushita, S. Yagami, A. Kato, H. Mitsuda, D. Aoki and K. Fukushima, *J. Agric. Food Chem.*, 2020, **68**, 9245–9251.

71 H. N. Lan, R. Y. Liu, Z. H. Liu, X. Li, B. Z. Li and Y. J. Yuan, *Biotechnol. Adv.*, 2023, **64**, 108107.

72 H. Liu, Z. H. Liu, R. K. Zhang, J. S. Yuan, B. Z. Li and Y. J. Yuan, *Biotechnol. Adv.*, 2022, **60**, 108000.

73 D. H. Jung, E. J. Kim, E. Jung, R. J. Kazlauskas, K. Y. Choi and B. G. Kim, *Biotechnol. Bioeng.*, 2015, **113**, 1493–1503.

74 Z. Chen, H. Liu, Q. J. Zong, T. X. Liang, J. Sun, T. Xu, Z. H. Liu, J. P. Wu, B. Z. Li and Y. J. Yuan, *ACS Sustainable Chem. Eng.*, 2024, **49**, 17726–17738.

75 S. Notonier, A. Z. Werner, E. Kuatsjah, L. Dumalo, P. E. Abraham, E. A. Hatmaker, C. B. Hoyt, A. Amore, K. J. Ramirez, S. P. Woodworth, D. M. Klingeman, R. J. Giannone, A. M. Guss, R. L. Hettich, L. D. Eltis, C. W. Johnson and G. T. Beckham, *Metab. Eng.*, 2021, **65**, 111–122.

76 R. K. Zhang, Y. S. Tan, Y. Z. Cui, X. Xin, Z. H. Liu, B. Z. Li and Y. J. Yuan, *Green Chem.*, 2021, **23**, 6515.

77 H. Liu, X. Tao, S. Ntakirutimana, Z. H. Liu, B. Z. Li and Y. J. Yuan, *Chem. Eng. J.*, 2024, **495**, 153375.

78 C. W. Johnson and G. T. Beckham, *Metab. Eng.*, 2015, **28**, 240–247.

79 L. G. Zou, Y. T. Yao, F. F. Wen, X. Zhang, B. T. Liu, D. W. Li, Y. F. Yang, W. D. Yang, S. Balamurugan and H. Y. Li, *J. Agric. Food Chem.*, 2023, **71**, 10065–10074.

80 D. R. Vardon, M. A. Franden, C. W. Johnson, E. M. Karp, M. T. Guarnieri, J. G. Linger, M. J. Salm, T. J. Strathmann and G. T. Beckham, *Energy Environ. Sci.*, 2015, **8**, 617–628.

81 M. Kohlstedt, S. Starck, N. Barton, J. Stolzenberger, M. Selzer, K. Mehlmann, R. Schneider, D. Pleissner, J. Rinkel, J. S. Dickschat, J. Venus, J. B. J. H. V. Duuren and C. Wittmann, *Metab. Eng.*, 2018, **47**, 279–293.

82 J. M. Perez, W. S. Kontur, M. Alhorech, J. Coplien, S. D. Karlen, S. S. Stahl, T. J. Donohue and D. R. Noguera, *Green Chem.*, 2019, **21**, 1340–1350.

83 C. W. Johnson, D. Salvachúa, P. Khanna, H. Smith, D. J. Peterson and G. T. Beckham, *Metab. Eng. Commun.*, 2016, **3**, 111–119.

84 R. Zhang, J. Wang, S. Milligan and Y. Yan, *Green Chem.*, 2021, **23**, 8238–8250.

85 W. Zeng, L. Guo, S. Xu, J. Chen and J. Zhou, *Trends Biotechnol.*, 2020, **38**, 888–906.

86 A. Nakamura, N. Honma, Y. Tanaka, Y. Suzuki, Y. Shida, Y. Tsuda, K. Hidaka and W. Ogasawara, *Anal. Chem.*, 2022, **94**, 2416–2424.

87 M. Klaus, P. J. Zurek, T. S. Kaminski, A. Pushpanath, K. Neufeld and F. Hollfelder, *ChemBioChem*, 2021, **22**, 3292–3299.

88 B. Kintses, C. Hein, M. F. Mohamed, M. Fischlechner, F. Courtois, C. Lainé and F. Hollfelder, *Chem. Biol.*, 2012, **19**, 1001–1009.

89 J. Panwar, A. Autour and C. A. Merten, *Nat. Protoc.*, 2023, **18**, 1090–1136.

90 Q. C. Xu, Z. O. Sebastian, G. Lindquist, H. Jiang, Ch. Z. Li and W. B. Shannon, *ACS Energy Lett.*, 2021, **6**, 305–312.

91 K. Radotić, A. Kalauzi, D. Djikanović, M. Jeremić, R. M. Leblanc and Z. G. Cerović, *J. Photochem. Photobiol. B*, 2006, **83**, 1–10.

92 G. Paës, *Molecules*, 2014, **19**, 9380–9402.

93 J. Arnthong, C. Siamphan, C. Chuaseeharonnachai, N. Boonyuen and S. Suwannarangsee, *J. Microbiol. Biotechnol.*, 2020, **30**, 1670–1679.

94 N. S. Ali, F. Huang, W. Qin and T. C. Yang, *Biotechnol. Rep.*, 2023, **39**, e00809.

95 R. Khandeparkar and N. B. Bhosle, *Res. Microbiol.*, 2006, **157**, 315–325.

96 Y. Ensari, G. V. Dhoke, M. D. Davari, A. J. Ruff and U. Schwaneberg, *ChemBioChem*, 2018, **19**, 1563–1569.

97 G. Yang and S. G. Withers, *ChemBioChem*, 2009, **10**, 2704–2715.

98 G. Körfer, V. Besirlioglu, M. D. Davari, R. Martinez, L. Vojcic and U. Schwaneberg, *Biotechnol. Bioeng.*, 2022, **119**, 2076–2087.

99 A. I. Vicente, J. V. Gonzalez, P. S. Moriano, C. M. Alvarez, A. O. Ballesteros and M. Alcalde, *J. Mol. Catal. B: Enzym.*, 2016, **134**, 323–330.

100 J. Xu, Y. Zhang, H. Yu, X. Gao and S. Shao, *Anal. Chem.*, 2015, **88**, 1455–1461.

101 L. G. Wang, M. He, X. W. Liu, L. J. Zhai, L. X. Niu, Z. L. Xue and H. T. Wu, *Green Chem.*, 2023, **25**, 550–553.

102 G. Sun, L. Qu, F. Azi, Y. Liu, J. Li, X. Lv, G. Du, J. Chen, C. H. Chen and L. Liu, *Biosens. Bioelectron.*, 2023, **225**, 115107.

103 R. He, R. Ding, J. A. Heyman, D. Zhang and R. Tu, *J. Ind. Microbiol. Biotechnol.*, 2019, **46**, 1603–1610.

104 B. Kintses, L. D. van Vliet, S. R. A. Devenish and F. Hollfelder, *Curr. Opin. Chem. Biol.*, 2010, **14**, 548–555.

105 J. J. Agresti, E. Antipov, A. R. Abate, K. Ahna, A. C. Rowat, J. C. Baret, M. Marquez, A. M. Klibanov, A. D. Griffiths and D. A. Weitz, *Proc. Natl. Acad. Sci. U. S. A.*, 2010, **107**, 6550.

106 H. Yuan, Y. Zhou, Y. Lin, R. Tu, Y. Guo, Y. Zhang and Q. Wang, *Biotechnol. Biofuels Bioprod.*, 2022, **15**, 50.

107 I. Swyer, R. Fobel and A. R. Wheeler, *Langmuir*, 2019, **35**, 5342–5352.

108 D. Hess, V. Dockalova, P. Kokkonen, D. Bednar, J. Damborsky, A. deMello, Z. Prokop and S. Stavrakis, *Chem.*, 2021, **7**, 1066–1079.

109 B. Sana, K. H. B. Chia, S. S. Raghavan, B. Ramalingam, N. Nagarajan, J. Seayad and F. J. Ghadessy, *Biotechnol. Biofuels*, 2017, **10**, 32.

110 S. Neun, P. J. Zurek, T. S. Kaminski and F. Hollfelder, *Methods Enzymol.*, 2020, **643**, 317–343.

111 S. Neun, P. Brear, E. Campbell, T. Tryfona, K. El Omari, A. Wagner, P. Dupree, M. Hyvonen and F. Hollfelder, *Nat. Chem. Biol.*, 2022, **18**, 1096–1103.

112 S. Neun, L. V. Vliet, F. Hollfelder and F. Gielen, *Anal. Chem.*, 2022, **94**, 16701–16710.

113 F. Gielen, T. Buryska, L. V. Vliet, M. Butz, J. Damborsky, Z. Prokop and F. Hollfelder, *Anal. Chem.*, 2015, **87**, 624–632.

114 Y. Cui, Y. Chen, X. Liu, S. Dong, Y. E. Tian, Y. Qiao, R. Mitra, J. Han, C. Li, X. Han, W. Liu, Q. Chen, W. Wei, X. Wang, W. Du, S. Tang, H. Xiang, H. Liu, Y. Liang, K. N. Houk and B. Wu, *ACS Catal.*, 2021, **11**, 1340–1350.

115 D. C. Miller, S. V. Athavale and F. H. Arnold, *Nat. Synth.*, 2022, **1**, 18–23.

116 C. Del Cerro, E. Erickson, T. Dong, A. R. Wong, E. K. Eder, S. O. Purvine, H. D. Mitchell, K. K. Weitz, L. M. Markillie, M. C. Burnet, D. W. Hoyt, R. K. Chu, J. F. Cheng, K. J. Ramirez, R. Katahira, W. Xiong, M. E. Himmel, V. Subramanian, J. G. Linger and D. Salvachua, *Proc. Natl. Acad. Sci. U. S. A.*, 2021, **118**, e2017381118.

117 C. C. Chen, L. Dai, L. Ma and R. T. Guo, *Nat. Rev. Chem.*, 2020, **4**, 114–126.

118 F. J. R. Duenas, M. Morales, E. Garcia, Y. Miki, M. J. Martinez and A. T. Martinez, *J. Exp. Bot.*, 2009, **60**, 441–452.

119 M. P. Boada, F. J. R. Dueñas, R. Pogni, R. Basosi, T. Choinowski, M. Jesús Martínez, K. Piontek and A. T. Martínez, *J. Mol. Biol.*, 2005, **354**, 385–402.

120 J. Jumper, R. Evans, A. Pritzel, T. Green, M. Figurnov, O. Ronneberger, K. Tunyasuvunakool, R. Bates, A. Žídek, A. Potapenko, A. Bridgl, C. Meyer, S. A. A. Kohl, A. J. Ballard, A. Cowie, B. R. Paredes, S. Nikolov, R. Jain, J. Adler, T. Back, S. Petersen, D. Reiman, E. Clancy, M. Zielinski, M. Steinegger, M. Pacholska, T. Berghammer, S. Bodenstein, D. Silver, O. Vinyals, A. W. Senior, K. Kavukcuoglu, P. Kohli and D. Hassabis, *Nature*, 2021, **596**, 583–589.

121 A. Goldenzweig, M. Goldsmith, S. E. Hill, O. Gertman, P. Laurino, Y. Ashani, O. Dym, T. Unger, S. Albeck, J. Prilusky, R. L. Lieberman, A. Aharoni, I. Silman, J. L. Sussman, D. S. Tawfik and S. J. Fleishman, *Mol. Cell*, 2016, **63**, 337–346.

122 S. B. Zucker, V. Mindel, E. G. Ruiz, J. J. Weinstein, M. Alcalde and S. J. Fleishman, *J. Am. Chem. Soc.*, 2022, **144**, 3564–3571.

123 D. Salvachúa, C. W. Johnson, C. A. Singer, H. Rohrer, D. J. Peterson, B. A. Black, A. Knapp and G. T. Beckham, *Green Chem.*, 2018, **20**, 5007–5019.

124 G. T. Beckham, C. W. Johnson, E. M. Karp, D. Salvachúa and D. R. Vardon, *Curr. Opin. Biotechnol.*, 2016, **42**, 40–53.

125 M. M. Machovina, S. J. B. Mallinson, B. C. Knott, A. W. Meyers, M. G. Borràs, L. Bu, J. E. Gado, A. Oliver, G. P. Schmidt, D. J. Hinchen, M. F. Crowley, C. W. Johnson, E. L. Neidle, C. M. Payne, K. N. Houk, G. T. Beckham, J. E. McGeehan and J. L. DuBois, *Proc. Natl. Acad. Sci. U. S. A.*, 2019, **116**, 13970–13976.

126 E. S. Ellis, D. J. Hinchen, A. Bleem, L. Bu, S. J. B. Mallinson, M. D. Allen, B. R. Streit, M. M. Machovina, Q. V. Doolin, W. E. Michener, C. W. Johnson, B. C. Knott, G. T. Beckham, J. E. McGeehan and J. L. DuBois, *JACS Au*, 2021, **1**, 252–261.

127 Z. Li, Y. Jiang, F. P. Guengerich, L. Ma, S. Li and W. Zhang, *J. Biol. Chem.*, 2020, **295**, 833–849.

128 S. J. B. Mallinson, M. M. Machovina, R. L. Silveira, M. G. Borràs, N. Gallup, C. W. Johnson, M. D. Allen, M. S. Skaf, M. F. Crowley, E. L. Neidle, K. N. Houk, G. T. Beckham, J. L. DuBois and J. E. McGeehan, *Nat. Commun.*, 2018, **9**, 2487.

129 M. Ahmad, J. N. Roberts, E. M. Hardiman, R. Singh, L. D. Eltis and T. D. H. Bugg, *Biochemistry*, 2011, **50**, 5096–5107.

130 V. Brissos, D. Tavares, A. C. Sousa, M. P. Robalo and L. O. Martins, *ACS Catal.*, 2017, **7**, 3454–3465.

131 R. R. Pour, A. Ehibatiomhan, Y. Huang, B. Ashley, G. M. Rashid, S. M. Williams and T. D. H. Bugg, *Enzyme Microb. Technol.*, 2019, **123**, 21–29.

132 A. Arias, G. Feijoo and M. T. Moreira, *Environ. Technol. Innov.*, 2023, **32**, 103277.

133 M. Liao and Y. Yao, *GCB Bioenergy*, 2021, **13**, 774–802.

134 N. Prioux, R. Ouaret, G. Hetreux and J. P. Belaud, *Clean Technol. Environ.*, 2023, **25**, 689–702.

135 D. S. Vilar, M. Bilal, R. N. Bharagava, A. Kumar, A. Kumar Nadda, G. R. S. Banda, K. I. B. Eguiluz and L. F. R. Ferreira, *J. Chem. Technol. Biotechnol.*, 2021, **97**, 327–342.

136 A. K. Singh, M. Bilal, H. M. N. Iqbal and A. Raj, *Int. J. Biol. Macromol.*, 2021, **177**, 58–82.

137 M. Bilal and H. M. N. Iqbal, *Catal. Lett.*, 2020, **150**, 524–543.

138 S. S. Hernández, C. V. Ayala, P. L. I. Flores, M. J. R. Alanis, R. P. Saldivar, H. M. N. Iqbal and D. C. Nieves, *Int. J. Biol. Macromol.*, 2020, **161**, 1099–1116.

139 A. K. Singh, M. Bilal, H. M. N. Iqbal and A. Raj, *Sci. Total Environ.*, 2021, **770**, 144561.

140 A. K. Singh, S. K. Katari, A. Umamaheswari and A. Raj, *RSC Adv.*, 2021, **11**, 14632–14653.

141 A. K. Singh, M. Bilal, H. M. N. Iqbal and A. Raj, *Chemosphere*, 2022, **292**, 133250.

142 A. K. Singh, M. Bilal, T. Jasionowski and H. M. N. Iqbal, *Chemosphere*, 2023, **313**, 137546.

143 L. J. Wang, C. Xue, G. Owens and Z. L. Chen, *Bioresour. Technol.*, 2022, **345**, 126565.

144 C. D. Fernandes, V. R. S. Nascimento, D. B. Meneses, D. S. Vilar, N. H. Torres, M. S. Leite, J. R. V. Baudrit, M. Bilal, H. M. N. Iqbal, R. N. Bharagava, S. M. Egues and L. F. R. Ferreira, *J. Hazard. Mater.*, 2020, **399**, 153–181.

145 J. Yang, I. Anishchenko, H. Park, Z. Peng, S. Ovchinnikov and D. Baker, *Proc. Natl. Acad. Sci. U. S. A.*, 2020, **117**, 1496–1503.

146 T. H. Tsui, M. C. M. V. Loosdrecht, Y. Dai and Y. W. Tong, *Bioresour. Technol.*, 2023, **369**, 128445.

147 N. Hasegawa, M. Sugiyama and K. Igarashi, *BioRxiv*, 2024, **15**, 585254.

148 R. Jiang, L. Shang, R. Wang, D. Wang and N. Wei, *Environ. Sci. Technol. Lett.*, 2023, **10**, 557–564.

149 Y. L. Xiang, Y. B. Zhang, J. Q. Wu, J. Zhu, B. W. Cao and C. Y. Xiong, *Renewable Energy*, 2024, **235**, 121289.

150 J. Li, Z. Liu, J. Zhao, G. Wang and T. Xie, *Int. J. Biol. Macromol.*, 2024, **256**, 128487.

151 A. Manglesh, V. Kumar, D. Chandra, V. Thakur, U. Sharma and D. Singh, *Int. J. Biol. Macromol.*, 2023, **234**, 123601.

152 P. Bhatt, K. Bhatt, W. J. Chen, Y. Huang, Y. Xiao, S. Wu, Q. Lei, J. Zhong, X. Zhu and S. Chen, *J. Hazard. Mater.*, 2023, **443**, 130319.

153 N. K. Chopra and S. Sondhi, *Int. J. Biol. Macromol.*, 2022, **206**, 1003–1011.

154 S. A. Mayr, R. Subagia, R. Weiss, N. Schwaiger, H. K. Weber, J. Leitner, D. Ribitsch, G. S. Nyanhongo and G. M. Guebitz, *Int. J. Mol. Sci.*, 2021, **22**, 13161.

155 L. Cao, L. Lin, H. Sui, H. Wang, Z. Zhang, N. Jiao and J. Zhou, *Green Chem.*, 2021, **23**, 2079–2094.

156 N. K. Kheti, S. Rath and H. Thatoi, *Sustainable Chem. Environ.*, 2023, **2**, 100009.

157 A. Singh, R. Kumar, A. Maurya, P. Chowdhary and A. Raj, *Biotechnol. Rep.*, 2022, **35**, e00755.

158 A. Alfi, B. Zhu, J. Damnjanovic, T. Kojima, Y. Iwasaki and H. Nakano, *J. Biosci. Bioeng.*, 2019, **128**, 290–295.

159 T. V. T. Nguyen, S. Kim, C. G. Yoo, J. W. Choi, G. Leem and Y. H. Kim, *ACS Catal.*, 2024, **14**, 11733–11740.

160 H. Gye, H. Baek, S. Han, H. Kwon, T. V. T. Nguyen, L. T. M. Pham, S. Kang, Y. H. Nho, D. W. Lee and Y. H. Kim, *Biomacromolecules*, 2023, **24**, 2633–2642.

161 D. Linde, I. A. Fernandez, M. Laloux, J. E. Aguiar-Cervera, A. L. de Lace, F. J. Ruiz-Duenas and A. T. Martinez, *Int. J. Mol. Sci.*, 2021, **22**, 2629.

162 S. I. Khan, N. S. Zada, M. Sahinkaya, D. N. Colak, S. Ahmed, F. Hasan, A. O. Belduz, S. Canakci, S. Khan, M. Badshah and A. A. Shah, *Enzyme Microb. Technol.*, 2021, **151**, 109917.

163 S. Ding, C. Lin, Q. Xiao, F. Feng, J. Wang, X. Zhang, S. Yang, L. Li and F. Li, *Sci. Total Environ.*, 2024, **908**, 168500.

164 S. Sethupathy, R. Xie, N. Liang, R. M. B. Shafreen, M. Y. Ali, Z. Zhuang, L. Zhe, Z. Zahoor, Y. C. Yong and D. Zhu, *Int. J. Biol. Macromol.*, 2023, **253**, 127117.

165 P. Dhankhar, V. Dalal, V. Singh, A. K. Sharma and P. Kumar, *Int. J. Biol. Macromol.*, 2021, **193**, 601–608.

166 K. S. K. Teo, K. Kondo, S. M. R. Khattab, T. Watanabe, T. Nagata and M. Katahira, *J. Agric. Food Chem.*, 2024, **72**, 2657–2666.

167 K. Saikia, D. Vishnu, A. K. Rathankumar, B. Palanisamy Athiyaman, R. A. Batista-Garcia, J. L. Folch-Mallol, H. Cabana and V. V. Kumar, *J. Air Waste Manage. Assoc.*, 2020, **70**, 1252–1259.

168 F. Li, F. Ma, H. Zhao, S. Zhang, L. Wang, X. Zhang and H. Yu, *Appl. Environ. Microbiol.*, 2019, **85**, e02803.